# Solid state $^{17}$O NMR—an introduction to the background principles and applications to inorganic materials

**Sharon E. Ashbrook[a] and Mark E. Smith*[b]**

***Received 2nd March 2006***
***First published as an Advance Article on the web 4th May 2006***
**DOI: 10.1039/b514051j**

Oxygen is a key chemical element and solid state NMR can provide unique insight into the its local environment. In the last decade there have been significant advances (sensitivity, resolution) in the NMR methodology for non-integer spin quadrupole nuclei such as oxygen and the background to these techniques is presented in this *tutorial review*. The information that the NMR parameters can provide about the local environment is explained through a series of illustrations from different areas of solid state chemistry and structural science of inorganic materials.

## 1. Introduction

Given the importance of oxide-based materials to technology (*e.g.*, advanced, structural and functional ceramics, catalysts, *etc.*), solid state chemistry and mineralogy, as well as being a key element in biomolecular chemistry, the spectroscopic study of oxygen is of fundamental importance. Many of the key questions concerning these areas require an understanding of the bonding, with oxygen usually appearing throughout or at key points in the structure. As nuclear magnetic resonance (NMR) is sensitive to short-range, atomic scale structure, through the interactions (*e.g.*, dipolar, chemical shielding, quadrupolar)[1] that affect NMR spectra, $^{17}$O NMR should be one of the key spectroscopic probes. However, until the last few years, $^{17}$O NMR reports from solids have been somewhat scarce compared to commonly studied nuclei such as $^{13}$C, $^{27}$Al and $^{29}$Si. The three stable isotopes of oxygen have natural abundances of $^{16}$O – 99.76%, $^{17}$O – 0.037% and $^{18}$O – 0.2%, but only $^{17}$O has a non-zero nuclear spin quantum number ($I$ = 5/2) and is therefore accessible to NMR. Hence, for routine observation isotopic enrichment is usually necessary, involving both cost and effort, which hindered the initial development of $^{17}$O NMR of solids. A second problem with $^{17}$O is the significant broadening which can affect the resonances of this

[a]*School of Chemistry, University of St Andrews and EaStCHEM, St Andrews, Fife, UK KY16 9ST*
[b]*Department of Physics, University of Warwick, Coventry, UK CV4 7AL. E-mail: M.E.Smith.1@warwick.ac.uk*

**Sharon E. Ashbrook**

*Sharon Ashbrook graduated in Chemistry from Hertford College, Oxford where she also gained her DPhil for work on new solid state NMR techniques for quadrupolar nuclei. After postdoctoral research at the University of Exeter (in the group of Dr Stephen Wimperis) she became a Teaching Fellow in Mineral Physics at the University of Cambridge. In 2003, she was awarded the Royal Society Dorothy Hodgkin Fellow at the Department of Earth Sciences, University of Cambridge and also held the Charles and Katherine Darwin Research Fellowship at Darwin College. From October 2005, she was appointed as an Academic Fellow in the School of Chemistry, University of St Andrews. Currently, she is interested in both the development of new techniques for solid state NMR and their applications, particularly to mineral systems and to ceramic phases for the encapsulation of nuclear waste. She is also interested in the use of first-principles calculations for the determination of NMR parameters. In 2004, Sharon was awarded the Royal Society of Chemistry Harrison Prize for her contributions to solid state NMR.*

**Mark E. Smith**

*Mark Smith graduated in Natural Sciences (Physics) from Churchill College, Cambridge and then completed a PhD on solid state NMR of ceramic phases in the Department of Physics, University of Warwick under the supervision of Prof. Ray Dupree. He subsequently held research posts with Bruker Analytische in Rheinstetten, Germany and the CSIRO Division of Materials Science and Technology, Melbourne, Australia. He returned to UK academic life as a Lecturer and then Reader in Solid State NMR at the University of Kent, Canterbury before moving back to Warwick where is now a Professor of Physics. He has wide ranging research interests in solid state NMR of inorganic materials, particularly those showing disorder, with a currently developing interest in the application of solid state NMR of quadrupole nuclei to biological systems. He has been a Royal Society Leverhulme Trust Senior Research Fellow, a past secretary of the BRSG: the Magnetic Resonance Group of the Institute of Physics and RSC reporter on Solid State NMR.*

 

quadrupole nucleus. There were a few early high resolution magic angle spinning (MAS) solid state $^{17}O$ NMR studies around 20 years ago; the first one published in 1983.[2] It became clear in the early work that the quadrupole interaction is a strong function of the 'covalency' of the M–O bond.[3] Many of these bonds can be highly ionic, but can still have a covalency associated with them. As a first approximation the quadrupole coupling constant ($\chi_Q$ see Sec 2.2) where there are just M–O bonds present can be estimated as

$$\chi_Q \text{ (in MHz)} = -0.203I(\%) + 14.78, \quad (1)$$

where $I$ is the ionicity of the M–O bond defined in terms of the Pauling electronegativities $EN$(M,O) as

$$I(\%) = 100[EN(O)–EN(M)]/EN(O). \quad (2)$$

For asymmetric M–O–M′ bonds the average ionicity of the two different bonds is employed, or indeed averaging all the direct oxygen contacts for higher coordinations. Historically, because of their widespread occurrence and importance silicates/aluminosilicates were amongst the first compounds studied by $^{17}O$ MAS NMR, but they turn out to be one of the toughest problems for $^{17}O$ NMR to tackle, as they often contain many crystallographically inequivalent sites, with relatively small chemical shift differences (covering a range of ~70 ppm), but have relatively large quadrupole interactions (~5 MHz). The residual second-order quadrupolar broadening under MAS (Sec. 2.2) meant that early 11.7 T $^{17}O$ MAS NMR spectra showed relatively little promise because of the lack of resolution, often detecting only broad, overlapping resonances from Si–O–Si and Si–O–Al, rather than resolving all the crystallographically inequivalent sites. In retrospect these early experiments gave an unduly pessimistic outlook on how valuable $^{17}O$ NMR is for a wide range of materials and molecules. $^{17}O$ essentially has only a moderate magnetic moment $-1.132$ J $T^{-1}$ so that it resonates at 5.775 MHz $T^{-1}$. It has only a relatively small quadrupole moment of $-25.56$ mbarns (a number of papers say $^{17}O$ has a moderately large quadrupole moment, but of the stable non-integer spin quadrupole nuclei only $^{95}Mo$ and $^{133}Cs$ have smaller values). However because of the only moderate Larmor frequency and substantial $\chi_Q$, often significant second-order quadrupole broadening occurs (see Sec. 2.2). $^{17}O$ generally has a large chemical shift range *e.g.*, $^{17}O$ in bonds to only titanium cover a shift range from 100 to 850 ppm, with respect to shift scale referenced to water at 0 ppm, thereby making it an attractive nucleus for solid state NMR, although there are some exceptions exemplified by the shift range of Si–O–Si only covering a range from 30 to 100 ppm. The late 1980s and 1990s brought great advances in the NMR methodology applicable to $^{17}O$, including a range of new techniques for more efficient narrowing of the quadrupole broadening, which are examined below. The last few years has seen a great increase in the number of papers reporting $^{17}O$ solid state NMR, giving the technique much more impetus as it has been demonstrated that $^{17}O$ NMR can provide key information about materials. The structure of this paper, in keeping with the spirit of a tutorial review, gives some of the background to the relevant NMR, followed by some examples of the applications to illustrate the novel information that the technique can provide. We feel it is important to give an introduction to the spectroscopy and hardware that makes $^{17}O$ solid state NMR a powerful structural probe, but the reader could move directly from the introduction to the illustrative applications (Sec. 3). This review concentrates on applications to inorganic materials, since $^{17}O$ NMR of organic solids was very recently reviewed.[4] A limited number of key references and recent examples are given, as well as some other reviews of specific aspects of the technique and applications of $^{17}O$ solid state NMR where reference to the wider primary literature can be found.

## 2. Background to technique developments

### 2.1 Enrichment schemes

To allow routine NMR observation of $^{17}O$ usually requires that isotopic enrichment is undertaken and a number of schemes have been developed, with further research into increasingly efficient schemes, some of which are now effectively routine. The two readily available $^{17}O$-labelled sources are $O_2$ and $H_2O$, with typical $^{17}O$-enrichment levels of 10–75 at% (= atomic percent). The enrichment level of choice for any given experiment is a compromise between cost and the required sensitivity. Our experience shows that 20 at% enrichment of the precursor provides sufficient sensitivity for 1D spectroscopy, so that at current prices 1 g of the labeled oxide product typically costs £50–100 to manufacture. For experiments with less efficient filling factors (*e.g.*, DOR, see Sec. 2.2) and especially two-dimensional (2D) experiments, higher enrichments (35–45 at% or above) are desirable.

Hydrolysis of a reactive precursor, such as a chloride or an alkoxide results in efficient incorporation of the oxygen label. After reaction, usually at or below room temperature, samples are heated either to remove organic products or allow reaction.[1] Recently some detailed considerations have been given as to other synthetic routes so that small amounts of reagents could be employed. As an example, $ZrW_2O_8$ could be prepared *via* reaction of the pre-enriched component oxides or *via* a hydrated intermediate.[5] Thought has to be given about the firing atmosphere as exchange can often result in the loss of the label and high purity nitrogen/argon are preferred.[6] For reactions at elevated temperature, the time spent at the elevated temperature should be kept to a minimum. The intensity of the oxygen signal gives an indication of the loss of label. Fig. 1 shows the loss of signal from a $ZrO_2$–$TiO_2$–$SiO_2$ xerogel sample with progressive heating to 250, 500 and 750 °C, each for 2 hours, producing finally 25 ± 3% of the signal compared to that from the original room temperature gel. This compares with 31 ± 3% if the sample is heated directly to 750 °C for 2 hours. Heating under air directly to 750 °C results in only 10 ± 3% of the original signal being observed. Other routes including reacting soluble salts to form insoluble hydroxides that are subsequently calcined, exchange of sparingly soluble carbonates *via* water, or direct reaction of some metals with water have all been reported.[1]

Gas exchange can be used to enrich many oxides, with the sample heated under vacuum to remove the oxygen and the system then back filled with $^{17}O$-labeled $O_2$ before cooling

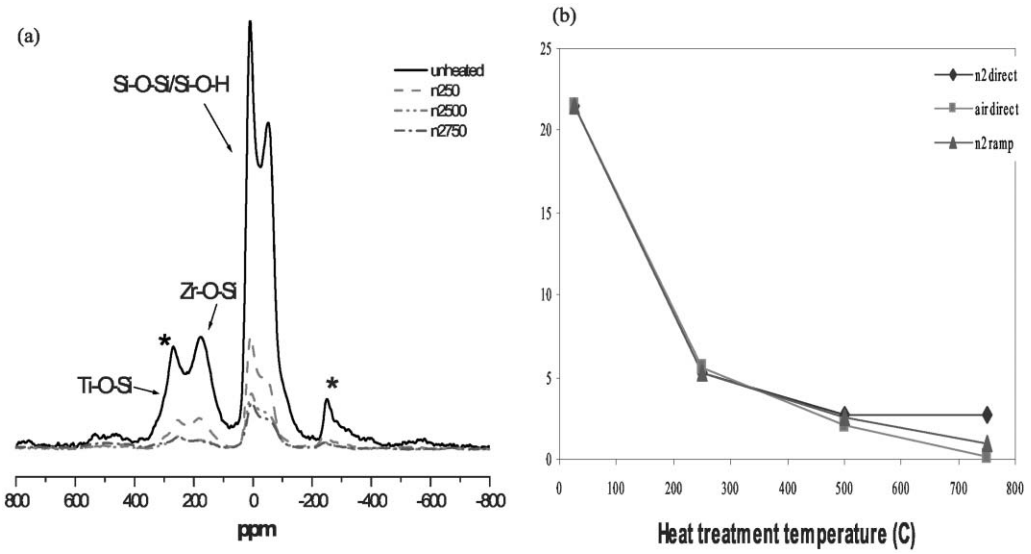


**Fig. 1** (a) Some representative $^{17}O$ MAS NMR spectra from a $ZrO_2$–$TiO_2$–$SiO_2$ xerogel sample after various heat treatments plotted on a normalised intensity scale and (b) comparison of the normalised integrated intensity of $^{17}O$ MAS NMR spectra after various heat treatments including directly heated to the target temperatures under nitrogen (upper) and air (middle) and successively to the different temperatures (lower). Reproduced from ref. 6, with permission of the copyright holder Elsevier Science.

back down to room temperature. This approach has now been widely used for enriching oxides, especially high temperature ceramic superconductors and zeolites. The kinetics of the exchange for microporous aluminosilicates has been studied in some detail when it was found that the rate of reaction was determined by the exchange step and not by diffusion in these usually fine grained materials. The different (Si,Al)–O–(Si,Al) fragments in zeolites are seen to exchange at different rates, with the difference in rates changing at different temperatures, hence care needs to be exercised that sufficient time is allowed for equilibrium to be established.

### 2.2 Physical background

NMR relies on the creation of a set of energy levels from the interaction between the large static magnetic field and the dipole moment of the nucleus—the Zeeman interaction, with the actual energy depending on the orientation of this magnetic dipole moment. In a quantum mechanical system for an $I = 5/2$ nucleus such as oxygen there will be $(2I + 1)$ orientations designated by the so-called magnetic quantum number $m$ (with $m = I, I - 1, \ldots -I$). This results in a set of energy levels ($E_m$) that are equally spaced as shown in Fig. 2(a), producing five transitions all at the same energy corresponding to the Larmor frequency ($\nu_0$), and hence a single resonance in the NMR spectrum (Fig. 2(b)).

The utility of NMR in providing information about the local surroundings comes from the other interactions that produce small changes (*i.e.*, perturbations) of the basic Zeeman ($E_m$) levels. Interactions with other surrounding magnetic moments usually produces dipolar broadening, whilst modifications of the actual field by the surrounding electronic charge cause chemical shifts. All nuclei experience these interactions, but nuclei with spin quantum number $I > 1/2$ have a non-spherical electrical charge distribution giving rise to an electric quadrupole moment, $eQ$. The interaction of this moment with the electric field gradient (EFG) present at the nucleus can often result in significant broadening of the NMR spectrum. This may at first sight appear surprising since it is an electrical interaction and NMR is a magnetic dipole spectroscopy. However, there is a dependence of this interaction on $m$, hence its influence on the NMR spectrum. The EFG varies in space and can be described by a tensor for which it is possible to define a principal axis system (PAS), *i.e.*, a frame where the tensor is diagonal, so that the EFG can be described by three components, $V_{xx}$, $V_{yy}$ and $V_{zz}$ where $|V_{zz}| \geqslant |V_{yy}| \geqslant |V_{xx}|$. In the literature it is not these three components that are usually reported, but rather the largest component of the EFG tensor $eq = V_{zz}$, and a cross-sectional shape, $\eta$, (the asymmetry parameter) where

$$\eta = \frac{(V_{xx} - V_{yy})}{V_{zz}} \tag{3}$$

such that $\eta$ lies between 0 (for an axially symmetric tensor) and 1. The magnitude of the quadrupolar interaction (the product of the EFG and quadrupole moment) is usually described by the quadrupolar coupling constant, which is a signed quantity that emerges from calculation, although experiments usually only produce the magnitude.

$$\chi_Q = \frac{e^2qQ}{h} \tag{4}$$

Note that once these two parameters have been determined experimentally the three components of the tensor are defined because the sum of the three must be identically zero. To understand the spectroscopic effects of the quadrupole interaction consider a spin system which is just the sum of the Zeeman and quadrupolar interactions. Although the quadrupolar interaction can be very large, it is usually much smaller than the Zeeman interaction (which is almost always the case for $^{17}O$) and its effect can therefore be described as a

 

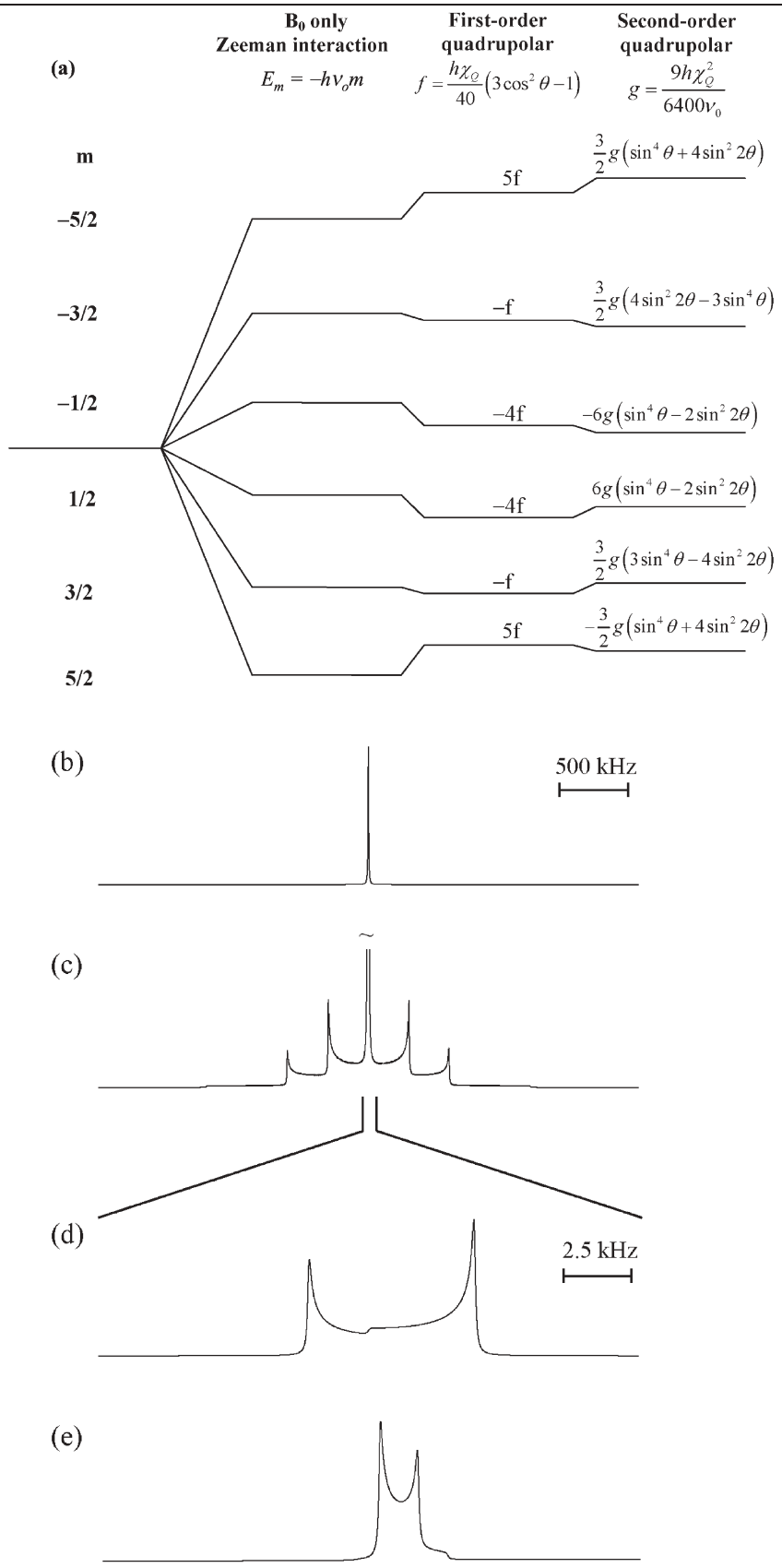


**Fig. 2** (a) Energy level diagram of an $I = 5/2$ nucleus showing the splitting due to the Zeeman interaction and then perturbed to first- and second-order by the quadrupole interaction (note the angular terms on the second-order term correct Fig. 2.8 in ref. 1 and Fig. 1(a) in ref. 7). SIMPSON simulations (b) static with no $\chi_Q$ and (c) static with $\chi_Q$, (d) static second-order central transition and (e) MAS second-order central transition with $\omega_R = 20$ kHz with $\chi_Q = 4$ MHz, $\eta = 0$ and $\delta_{iso} = 0$ ppm at a magnetic field of 14.1 T. Spectral widths are (b,c) 4 MHz and (d,e) 20 kHz. These spectra correspond to a sample with a unique oxygen site in a powder sample so that all orientations are present.

perturbation to the Zeeman energy levels, as shown in Fig. 2(a).[7] The effect of the quadrupolar interaction to a first-order approximation on the Zeeman energy levels is shown in Fig. 2(a) (for the case where $\eta = 0$). The central transition ($E_{1/2} \leftrightarrow E_{-1/2}$) is unaffected, remaining at $\nu_0$. However, the other transitions, termed satellite transitions, now possess frequencies which depend upon $\chi_Q$, resulting in a set of 5 effectively equally spaced resonances in the spectrum, whose intensities depend upon both $I$ and $m$. The satellite frequencies also depend upon the orientation of the quadrupolar PAS with respect to the magnetic field ($B_0$). For the case of $\eta = 0$, this dependence is given simply by $(3\cos^2\theta - 1)$. In a powdered sample, different crystallites possess different $\theta$ and a large anisotropic (or orientationally-dependent) spectral broadening is observed, as shown in Fig. 2(c), with a width proportional to $\chi_Q$ and a shape determined by $\eta$. The quadrupolar interaction can often be very large and spectra, as in Fig. 2(c), may be broadened over many MHz. In many cases, satellite transitions may be difficult, if not impossible, to observe and attention is usually focused upon the relatively sharp central transition.

When the quadrupolar interaction is very large such a first-order approximation is no longer sufficient to describe the spectrum and the effect of the quadrupolar interaction to second-order must be considered. This second-order term is more complicated, consisting of an isotropic (orientation-independent) shift, a second-rank broadening (proportional to $3\cos^2\theta - 1$) and a fourth-rank term which has a more complex orientational dependence.[7] As shown in Fig. 2(a), ($\eta = 0$) all transitions are affected by the second-order quadrupolar interaction, and have frequencies which depend upon both $\chi_Q$ and the orientation of the PAS. In this case, the central transition is no longer sharp but exhibits an anisotropic broadening in a powdered sample and is shifted from $\nu_0$ by the isotropic second-order quadrupolar shift, as shown in the expansion of the central-transition region of the spectrum in Fig. 2(d). The width of the resulting lineshapes depends principally (though not entirely) upon the magnitude of the interaction, proportional to $\chi_Q^2/\nu_0$ (hence the sign of $\chi_Q$ is lost), whilst the distinctive shape is determined by $\eta$. The second-order quadrupolar broadening is much smaller than the first-order broadening (directly proportional to $\chi_Q$), with $^{17}$O central-transition spectra often only a few tens of kHz wide.

It is well known in solid state NMR that the use of MAS, rapid spinning of the sample around an axis inclined at 54.736° to $B_0$, can increase spectral resolution. For spin $I = 1/2$ nuclei, MAS is able to produce high resolution spectra by removing dipolar interactions and chemical shift anisotropy (CSA), both proportional to $(3\cos^2\theta - 1)$, providing that the MAS rate is sufficiently fast. For quadrupolar nuclei, the presence of quadrupolar broadening poses an additional problem. MAS is able to remove completely the large first-order quadrupolar broadening (proportional to $3\cos^2\theta - 1$), increasing spectral resolution, but usually results in an extensive manifold of spinning sidebands, spaced at the spinning frequency around the centreband. However, when $\chi_Q$ is large and spectra exhibit second-order broadening, truly high resolution spectra are not achievable by MAS alone, due to the more complex orientational of second-order broadening. Only partial narrowing occurs under MAS and an anisotropic broadening remains in the spectrum, as in Fig. 2(e), with a shape determined by $\eta$.

Practical acquisition of quadrupole-broadened NMR spectra needs careful consideration, but is beyond the scope of this article; however summarising possible effects and important methods includes:[1,7]

• nutation effects of the magnetisation during the pulse that depend on $\chi_Q$,

• spectral distortion due to breadth of resonances, overcome by echo methods,

• transferring satellite-transition intensity into the usually observed central transition which includes rotor assisted population transfer (RAPT) which is applied to some examples in Sec. 3.2.

Also it is worth noting that Carr–Purcell–Meiboom–Gill (CPMG) echo trains (see also ref. 30), which are applicable to both spin-½ and quadrupole nuclei, can usefully provide significant signal enhancement.

An accurate determination of the quadrupolar (and chemical shift) parameters for individual species is often the aim of many experiments, as these values show a strong dependence upon the local chemical environment, providing useful structural information. In many cases, however, extraction of this detailed information is hindered by the presence of the second-order quadrupolar broadening, particularly if more than one chemically- or crystallographically-distinct species is present. The static $^{17}$O NMR spectra of the amino acid L-alanine at 14.1 and 8.45 T are shown in Fig. 3(a). $^{17}$O NMR spectra are referenced to the resonance from water at 0 ppm. That second-order quadrupole broadening is very important can be gauged by the decrease in width of the spectrum from ~1100 ppm to ~500 ppm as the field increases, not quite the inverse ratio of the fields squared of 2.78. This indicates that chemical shift anisotropy is making a significant contribution to the linewidth. The variation in lineshape also shows that sometimes at lower fields, although the lines are much broader, provided that they are not too broad to record, the different singularities may well be better separated. This is true for L-alanine which has two inequivalent oxygen sites. Fig. 3(b) shows the 14.1 T MAS NMR spectrum and significant narrowing of the resonances occurs. They still strongly overlap, although the singularities are well enough defined to allow simulation and analysis. Given the lack of complete resolution there is much interest in techniques which can either improve resolution, or produce truly high resolution (isotropic) spectra. These are not discussed in detail here and the reader is referred to recent reviews.[1,7] However, it is important that anyone contemplating observation has some awareness of the different approaches. Hence, these are listed here and summarised in Table 1 along with practical consequences for implementing the method.

1. One dimensional MAS observation of the satellite transitions ($m = \pm 3/2 \leftrightarrow \pm 1/2$) where the residual second-order broadening is significantly reduced for $I = 5/2$ to only ~0.29 of that of the central transition.

2. Double rotation (DOR) about two angles (usually 54.736° and 30.12°) simultaneously through the use of a sophisticated double rotor, removing both second- and fourth-rank broadenings to produce a truly high resolution spectrum.

 

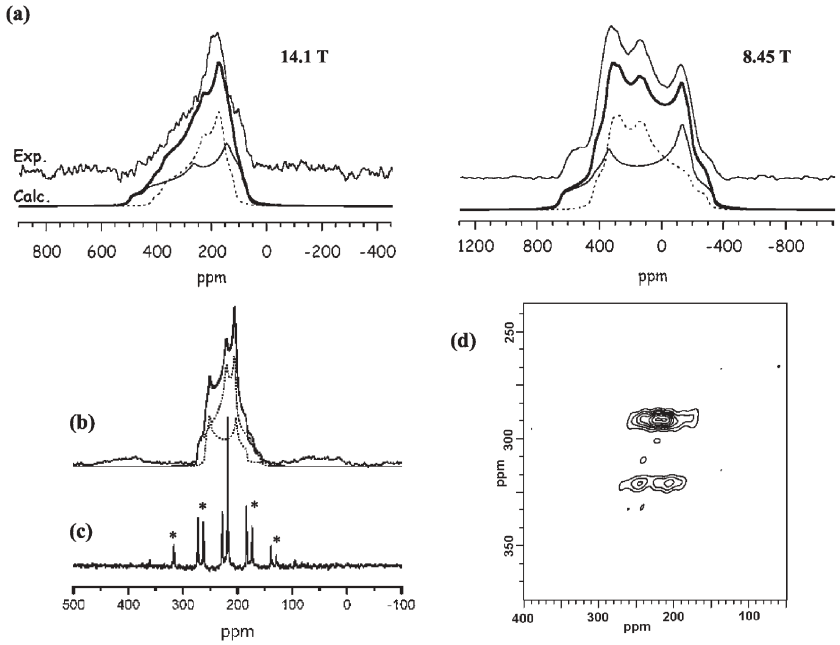


**Fig. 3** $^{17}$O NMR spectra from the amino acid L-alanine where there are two oxygen sites with $\chi_Q = 7.86 \pm 0.10$ MHz, $\eta = 0.28 \pm 0.10$ and $\delta_{iso} = 284.0 \pm 1$ ppm and $\chi_Q = 6.53 \pm 0.1$ MHz, $\eta = 0.70 \pm 0.10$ and $\delta_{iso} = 260.5 \pm 1$ ppm, respectively. (a) Static spectra at 14.1 and 8.45 T, and high resolution spectra at 14.1 T (b) MAS, (c) DOR and (d) 3Q MAS. The figures are reproduced with permission of the copyright owner the American Chemical Society, from ref 18 for (a) and 8 for (b) and (c).

3. Dynamic angle spinning (DAS) around two different angles sequentially in a 2D experiment.

4. Two-dimensional correlation techniques such as multiple-quantum (MQ) or satellite-transition (ST) MAS,[9] where removal of the anisotropic quadrupolar broadening is achieved through the correlation of either symmetric ($+m \leftrightarrow -m$) MQ transitions or single-quantum satellite transitions, with the single-quantum central-transition under MAS.

DOR offers perhaps the conceptually simplest approach to producing an isotropic spectrum, with good sensitivity in a one-dimensional experiment. The $^{17}$O DOR spectrum of L-alanine is shown in Fig. 3(c), where two sharp resonances can be identified along with spinning sidebands (denoted *). The narrowing under DOR compared to MAS is very marked, nearly a factor of 200 for L-alanine. The $^{17}$O 3Q MAS NMR spectrum of the same L-alanine sample (Fig. 3(d)) shows that again the two distinct resonances are observed and completely resolved.

The utility of MQ MAS techniques for $^{17}$O is reflected in the number of studies that now employ this approach and several illustrative examples are given in Sec. 3, so a brief explanation of the nature of this data and the extraction of NMR parameters is now given. Removal of the anisotropic quadrupolar broadening occurs in the 2D spectrum produced, which consists of ridges of intensity in the 2D dataset. The direction of these ridges depends on the actual pulse sequence used, the MQ transition observed (for $^{17}$O, this could be 3Q or 5Q) and the processing (*e.g.* whether a shearing transformation has been applied).[1,7] Along each ridge the quadrupolar information is retained through a typical MAS lineshape, from which $\chi_Q$ and $\eta$ may be extracted separately, along with $\delta_{iso}$. In cases where well-defined lineshapes are not observed in the anisotropic direction, information is still available from the position of the centre-of-gravity of a resonance, which depends on both the isotropic chemical shift, $\delta_{iso}$, and a quadrupolar shift (proportional to $P_Q = \chi_Q (1 + \eta^2/3)^{1/2}$). Spectra produced by projection perpendicular to the ridges show high resolution, *i.e.*, the second-order quadrupolar broadening is removed, with the resonance positions also defined by a combination of these shifts. There are a number of possible ways in which the chemical shift referencing in the second or $\delta_1$ dimension

**Table 1** Summary of experimental approaches for $^{17}$O NMR

| | Probe | Resolution | Considerations |
|---|---|---|---|
| Static | Static | Low | May require echo experiments but is relatively straightforward to implement |
| MAS | MAS | Good | Better sensitivity and resolution than static |
| DOR | Specialist | Excellent | Limited MAS rates, a 1D experiment, good sensitivity, but needs high degree of skill to spin |
| DAS | Specialist | Excellent | A 2D experiment, can be limited by $T_1$ particularly if MAS detected |
| MQMAS | MAS | Excellent | A 2D experiment relatively straightforward to use but has reduced sensitivity, particularly for high $\chi_Q$ |
| STMAS | MAS | Excellent | A 2D experiment, better sensitivity than MQ but does require accurate magic angle and highly stable MAS rate |

(*i.e.*, the multiple-quantum dimension) can be carried out. One approach involves referencing with respect to the conventional Larmor frequency, as in a conventional MAS spectrum, noting that shifts will appear a factor of 3 (for 3Q) or 5 (for 5Q) times larger than in the $\delta_2$ dimension. An alternative approach involves referencing to either 3 (3Q) or 5 (5Q) times the Larmor frequency, ensuring that resonances appear at similar shifts in 3Q or 5Q experiments. With both approaches care should be taken if a shearing transformation has been applied as $\delta_2$ now contains a mixture of single- and multiple-quantum shifts. More detailed descriptions of referencing in this case can be found in the literature. MQMAS can be easily implemented using a conventional MAS probe, but sensitivity is often compromised as filtration through MQ coherences is inherently inefficient. 3Q observation is more common than 5Q as excitation of the former is more efficient, resulting in better sensitivity. Quantitative interpretation of MQ data should, therefore, be approached with caution.

Although the acquisition of high resolution NMR spectra is important (and sometimes crucial), solid state $^{17}$O NMR spectra also contain a variety of additional information. One interaction of particular interest is the dipolar interaction which, owing to its strong dependence upon internuclear distances, is able to offer information on spatial proximity. The dipolar coupling is commonly exploited in the cross-polarisation (CP) experiment, a technique used widely in spin $I = 1/2$ NMR both to enhance sensitivity and extract distance information. The CP spectrum is therefore edited, with only oxygens sufficiently close in space to $^1$H appearing, aiding both spectral interpretation and assignment.[10] For quadrupolar nuclei, signal enhancement by CP is not common owing to the difficulties for parts of the CP experiment under MAS caused by the quadrupolar interaction. A range of ingenious recoupling experiments have been devised to exploit the dipolar coupling (and other couplings) and although these have yet to find widespread use for $^{17}$O some exciting possibilities exist and increasing use will be found. Applications of some of these are discussed Sec. 3.

### 2.3 Developments in NMR hardware and spectral analysis

The great increase in $^{17}$O NMR studies has been partially motivated by the availability of various pieces of equipment that have improved the quality of $^{17}$O NMR spectra. MAS is now much more routinely available above 25 kHz, with rotors (typically 2.5–4 mm diameter) that can contain sufficient sample to make collection times feasible. The availability of high magnetic fields *e.g.*, $\geqslant$14.1 T has meant that even oxygen sites with quite large $\chi_Q$ can be observed. To be ideally equipped a range of magnetic fields is extremely desirable. For materials where chemical shift dispersion is the dominant line broadening (*i.e.*, ionic M–O bonds in a disordered material) then medium fields (7.05–9.4 T) are ideal. For materials such as silicates and aluminosilicates where there are overlapping second-order quadrupole lineshapes and a relatively limited chemical shift range and chemical shift dispersion is a minor line broadening contribution, then higher magnetic fields are usually more suitable. In many cases to be able to extract information more unequivocally, collecting data at several fields can separate interactions due to their differing field dependencies.

The advent of genuinely high resolution techniques beyond MAS for non-integer spin quadrupolar nuclei has been important in the development of $^{17}$O NMR. For MQ work it is usually a 3Q experiment that is typically carried out with a 3.2 or 4 mm probe. The limiting factor is often the generation of sufficient rf field (which is a combination of the coil diameter and the voltage applied to the coil). It is limitations of the rf power that also mean that 5Q experiments are not more widely performed. The other higher order averaging techniques also have a role to play, although DAS probes are particularly rare. There are also still relatively few DOR probes, but there have been great improvements in the technology since the original designs when typical outer speeds of only 1 kHz were possible and stability meant that run times were only short. Now the rotor pressures are under computer control, and outer rotor speeds up to $\sim$2 kHz with essentially continuous operation possible. $^{17}$O is an ideal candidate for such high resolution approaches. For crystalline materials where $\chi_Q$ is quite large DOR can cause very significant narrowing compared to MAS, as was shown above for L-alanine.

Once spectra have been obtained then spectral analysis is required to extract the NMR interaction parameters. There has been great progress in the development of software for such analysis. For direct spectral simulation the dmfit program is user friendly and now widely used,[11] and the STARS program is also available. Another powerful program that allows the influence of experimental parameters such as pulse width, recycle delay, finite spinning speed, *etc.* to be taken into account is SIMPSON, and this allows optimum experimental conditions to be chosen.[12]

### 2.4 Calculations of NMR interaction parameters

The objective of many NMR experiments is to provide an insight into the local structural environment. Therefore, much work has focused on the dependence of NMR interactions upon a variety of structural parameters, including coordination number, bond distances and bond angles, with the ultimate aim of providing structural information *via* NMR spectra from unknown materials. Such correlations may be demonstrated empirically, through experiments on a series of related materials. More recently, the development of computational methods has provided an alternative, more flexible, and perhaps more detailed approach, also aiding in the assignment of complex spectra.

The quantum-mechanical calculation of NMR parameters involving a detailed description of the electrons and nuclei and the way they respond to the presence of a magnetic field, is a complex, many-body problem that cannot be solved without some approximations.[13] One approach is Hartree–Fock (HF) theory, where each electron is assumed to move independently in the mean field generated by the other electrons. Alternatively, density functional theory (DFT) can be employed where the energy is considered as a functional of the total charge density, thereby reducing significantly the dimensionality of the problem, but requiring additional

 

approximations and/or assumptions in nature of the functional used to describe electron exchange and correlation. DFT, however, has been used with great success, enabling calculations to be performed at fractions of the computational cost.

The simplest calculations of NMR parameters, using either HF or DFT, often with localised basis sets, such as the atomic orbitals, are performed for molecules. An infinite periodic solid is approximated only as a cluster, with the nucleus of interest at its centre,[13] and terminated with nuclei such as $^{1}$H. As the cluster size increases the calculated values approach those expected for an infinite solid. Tossell and co-workers were amongst the first to use the cluster method for the calculation of NMR parameters, with a recent example illustrating an application to $^{17}$O.[14] It can be difficult to achieve sufficiently large clusters and basis sets, restricting the accuracy of this type of calculation in many non-molecular solids. Qualitative results may be produced easily and are often sufficient for structural assignment of simple spectra. Furthermore, the variation of NMR parameters with structural features which depend primarily upon the local environment, can provide insight into related materials with more complex structures. As an example, work of Grandinetti and co-workers has utilised this cluster approach (along with more complex approaches) to calculate $^{17}$O NMR parameters, elucidating the changes in bond angle and the interaction with cations in silicate and aluminosilicate glasses (see Sec. 3.4)

However, in some cases the level of accuracy achieved by cluster methods is not sufficient for complete spectral assignment, as demonstrated by Bull *et al.* in their study of the zeolite ferrierite.[15] In this case, the many $^{17}$O species possess very similar NMR parameters and although important information is obtained, a full assignment of the $^{17}$O NMR spectrum is not possible by this method. Alternative approaches to the calculation of infinite solids often involve the use of periodic boundary conditions, exploiting the high translational symmetry of solids.[13] Although this approach formally applies only to perfect crystals, aperiodicity may be considered through the use of super cells. Many such codes use plane waves as basis sets. Although a large number of waves may be required to accurately represent complex wavefunctions, plane waves provide an orthonormal basis set which is computationally simple and cheap.

The WIEN code (an augmented plane wave code) has allowed the accurate determination of electric field gradient (EFG) tensors in many periodic crystals, aiding spectral assignment.[16] WIEN, an all-electron approach, is very accurate but time consuming. More recently, Pickard and Mauri introduced a plane wave pseudopotential method[13] for calculating NMR parameters, where the core and valence electrons are considered separately, an approximation which works well for many cases. This considerably improves the efficiency of the calculation allowing more complex systems to be calculated on reasonable timescales. An extension of this theory, the gauge including projector augmented wave (GIPAW) method,[13] 'reintroduces' the core electrons, allowing parameters dependent upon them, such as the chemical shift, to be determined. Since its introduction, the accuracy of this approach has been demonstrated in a variety of applications. For example, calculation of $^{17}$O quadrupole and chemical shift parameters enabled a full assignment of the ten oxygen species in the zeolite ferrierite.[13] In addition, the calculated parameters for a variety of silica polymorphs were shown to be in excellent agreement with experimental data, unlike many of the cluster calculations performed previously.[13] An additional study of calcium aluminosilicate minerals demonstrated that the partially covalent nature of the Ca–O bond had a considerable impact upon the $^{17}$O chemical shifts.[17] A further example of such calculations is of the $^{17}$O parameters in amino acids which showed that the $^{17}$O NMR interaction parameters were the most sensitive of any nucleus to changes of structure and also revealed a correlation between these parameters and hydrogen bonding.[18] With more examples of its utility appearing in the literature all the time, this method appears to offer an accurate, yet computationally efficient approach to the calculation of $^{17}$O NMR parameters for infinite solids.

## 3. Applications of $^{17}$O solid state NMR

### 3.1 Crystalline ionic oxides

For ionic oxide materials really quite high resolution $^{17}$O NMR spectra can be achieved by MAS alone as the electric field gradients, which are dominated by the local electron density, tend to be small.[3] As an example, variable field NMR clearly indicates that for all sites bonded only to titanium, the spectra are dominated by chemical shift effects with, in most cases, no real contribution from quadrupole effects. Often the relatively narrow MAS lines mean that even natural abundance work on such materials can be contemplated.[19] Some NaCl-structured oxides (*e.g.*, MgO, CaO) produce very narrow resonances that can be used as secondary shift references. In such oxides oxygen can often take a large range of coordination numbers (typically 1–5), with the $^{17}$O chemical shift becoming more shielded with increasing coordination number. From a number of studies $OTi_x$ coordinations have shifts in the range from 650 to 850 ppm for $x = 2$, from 450 to 650 ppm for $x = 3$, from 250 to 450 ppm for $x = 4$ and are seen at $<$250 ppm for $x = 5$. The total shift range covered by these units is almost 800 ppm, with also large changes in the chemical shift anisotropy (CSA). The sensitivity of the $^{17}$O chemical shift to the local bonding can be gauged through the three polymorphs of $TiO_2$, with all resonances being spread over a shift range of 35 ppm. These materials are all made up of $TiO_6$ units with the oxygens in $OTi_3$ coordinations. The polymorphs are structurally distinguished through slight differences in the ways the $TiO_6$ units are joined (*i.e.*, Ti–O–Ti bond angles). The solid state conversion of anatase to rutile can be followed through the two shifts being separated by $\sim$35 ppm and the structurally more distorted $TiO_6$ in rutile showing a small but noticeable $\chi_Q$. Hence, both the isotropic and anisotropic contributions to the interactions can be used to discriminate environments.

$^{17}$O MAS NMR spectra of ionic ternary oxygen-containing materials show a large variation in linewidth, with some spectra showing extremely high resolution revealing small shift differences from very subtle differences in the bonding around the oxygen site. A selection of typical spectra of titanates and zirconates that illustrate the variation in the number of resonances and the splitting are shown in Fig. 4. For $A_xBO_y$

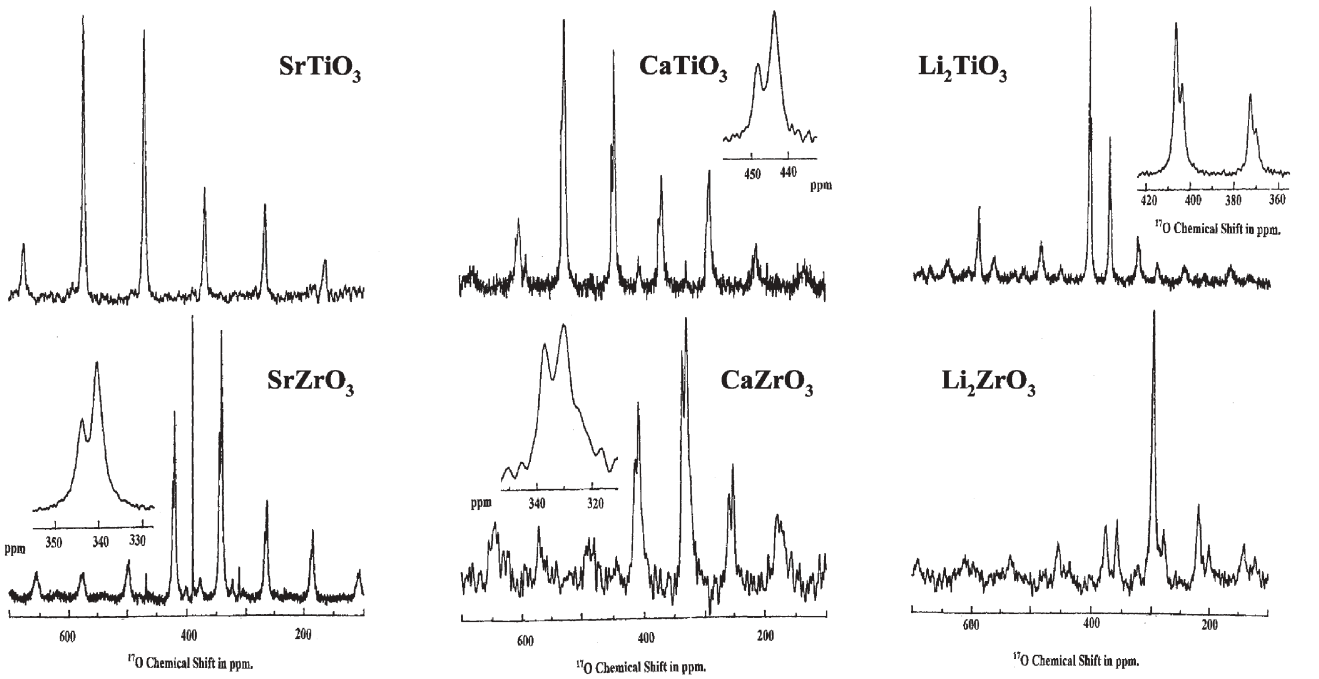


**Fig. 4** Typical $^{17}O$ MAS NMR spectra from some ionic titanates and zirconates showing the high resolution that is available under MAS alone in crystalline solids when the quadrupole interaction is small. Reproduced from ref. 20 with permission of the copyright owner the American Chemical Society.

compounds there are now increasingly large data sets of $^{17}O$ isotropic chemical shifts, with for example $^{17}O$ shift ranges of titanates (from 372 to 564 ppm), zirconates (from 298 to 376 ppm) and hafnates (from 237 to 332 ppm). This clearly indicates that the B ions principally determine these shift ranges for $^{17}O$. Comparison of isostructural zirconates and hafnates shows that the ratio of the isotropic shifts for $^{17}O$ (Hf/Zr) falls in the very narrow range 0.84–0.88, close to the ratio of the polarising powers of these two elements.[20] Cubic perovskites show only a single sharp oxygen resonance, reflecting the equivalence of all the oxygen sites in the structure. The splitting into two resonances in materials such as $CaTiO_3$ with the $GdFeO_3$-structure where oxygen sites become inequivalent is typically 5 ppm. In monoclinic materials of lower symmetry still (*e.g.*, $Li_2TiO_3$) there are only two different $^{17}O$ NMR signals, but these are now separated by greater shift differences (*e.g.*, $\sim$20 ppm).[20] A number of materials in such systems are important technologically, for instance as non-linear optical, ferroelectric and relaxor phases. In $KTiOPO_4$ two distinct classes of oxygen exist. One group links the $TiO_6$ and $PO_4$ units (*i.e.*, bridging oxygens (bo) Ti–O–P) and have $\chi_Q \sim 5$ MHz and shift range from 100 to 150 ppm. The second group is the non-bridging oxygens (nbo) that correspond to short Ti–O bonds, which are very much more ionic so have a smaller $\chi_Q$ ($\sim$1 MHz) but are markedly shifted at $\sim$750 ppm.[21] The $^{17}O$ CSA values for such compounds can also be readily characterised, again illustrating that the chemical shift interaction dominates the spectrum. The widths of $^{17}O$ CS tensors (technically termed the span) of titanates tend to spread over larger ranges of shift than for zirconates, reflecting the influence of the B cation on the CS tensor.

Oxygen ion motion is important in a number of key technological applications of oxides such as solid electrolytes and oxygen sensors, and is often also at the heart of negative thermal expansion behaviour. The oxygen motion in such materials can be readily studied by $^{17}O$ NMR. The number of spectral lines and changes in lineshape can be used to give an indication of the oxygen motion. For example, $Ba_2In_2O_5$ has three inequivalent oxygen sites within the orthorhombic structure at room temperature, with the population of mobile anions increasing until a single Lorentzian resonance is observed using variable high temperature $^{17}O$ NMR. Despite the number of such studies using $^{17}O$ being relatively few, in the last $\sim$3–4 years there has been a significant increase in such work, with detailed reports being produced for $BiMeVO_x$, $ZrW_2O_8$ and $La_2Mo_2O_9$. As an example, $ZrW_2O_8$ at room temperature exhibits 3 distinct resonances, corresponding to the 4 different oxygen sites.[22] As the temperature is raised the peaks broaden and then merge into a single, Lorentzian-like line, with a position close to the weighted mean of the room temperature isotropic positions (Fig. 5(a)) indicating that all the oxygen sites are involved in the exchange process. The changes in the spectra themselves do not reveal the mechanism of the exchange process in detail. To provide more detail 2D correlation experiments such as the 2D EXSY experiment, which shows exchange between sites through the appearance of cross-peaks linking the isotropic peaks on the diagonal (Fig. 5(b)), can be used. For $ZrW_2O_8$ cross peaks between all peaks on the diagonal occur so that all oxygens are participating in the exchange process, enabling discrimination of the competing models. By combining NMR data, such as the relaxation times and cross peak intensities, quantification of the rate constants for exchange is possible, and hence by

 

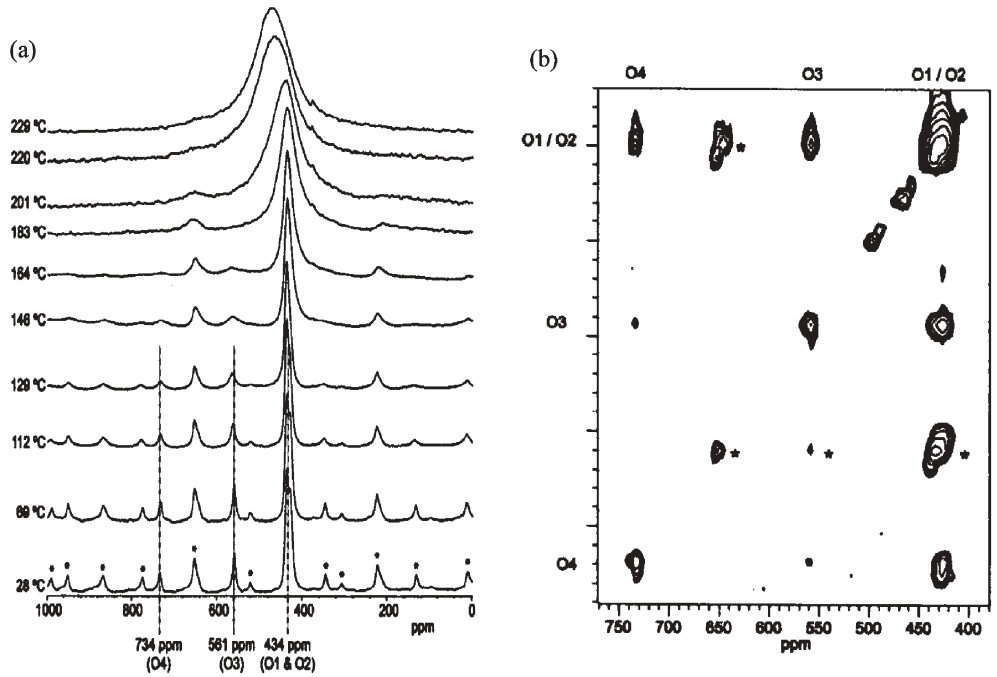


**Fig. 5** (a) Variable temperature $^{17}O$ MAS NMR spectra of $ZrW_2O_8$ and (b) 2D EXSY experiments with the diagonal showing the isotropic spectrum and off-diagonal cross peaks indicating which sites are exchanging. Reproduced from ref. 22 with permission of the copyright owner the Royal Society of Chemistry.

using variable temperature, activation energies for the different motions can be deduced. For $ZrW_2O_8$ analysis of the combined data set showed that the activation energy changed across the order/disorder transition.[23]

### 3.2 $^{17}O$ NMR in the earth sciences

Oxygen is the most abundant anion on Earth (30% by weight) and is a vital component of the silicate minerals which make up the Earth's crust and mantle. Oxygen NMR, therefore, appears to offer an unparalleled probe of the local structure and dynamics of many of the important materials which determine the physical and chemical properties of our planet. Despite this, relatively little $^{17}O$ NMR (compared to $^{27}Al$ or $^{29}Si$, for example) has been reported. The Earth's crust is composed principally of aluminosilicate minerals, whilst the mantle is predominantly magnesium silicate. Silicate structures tend to be dominated by the $SiO_4$ unit. These may be isolated from each other, coordinated to other cation polyhedra present in the structure. Alternatively, $SiO_4$ units can be connected by corner sharing, forming $Si_2O_7$ groups or chains. Further polymerisation results in silicate sheets or three-dimensional silicate frameworks. As the silicons form bo, $^{17}O$ $\chi_Q$ values of $\sim$4–6 MHz are observed, which are significantly higher than those for nbo.

Early MAS and static $^{17}O$ NMR[24] showed the presence of both bo and nbo in alkaline earth chain silicates, demonstrating also a dependence of both the chemical shift and quadrupolar coupling upon the nature of the cation present, although as discussed above, the low resolution of these techniques hindered extraction of detailed information, including in some cases, the exact number of distinct species present. However, well-crystalline silicate minerals are excellent candidates for high resolution techniques, and many more studies have resulted.

From a chemical perspective, perhaps the simplest 'silicates' are the silica polymorphs themselves. All consist of three-dimensional frameworks formed by corner-sharing $SiO_n$ units, but exhibit a range of structure types, providing an ideal system for determining the effect of structural, rather than chemical changes, upon the $^{17}O$ NMR parameters. In these frameworks all oxygen species are bridging (Si–O–Si) and possess large $\chi_Q$, usually 5–6 MHz. Quartz and cristobalite possess only one distinct oxygen enabling NMR parameters to be determined directly from one-dimensional static and MAS experiments. Coesite, however, possesses five similar oxygen species, preventing such a simple analysis. Grandinetti *et al.*[25] utilised a 15 day DAS experiment to resolve these distinct species. In contrast to the other polymorphs, stishovite, a high-pressure polymorph, contains corner-sharing $SiO_6$ octahedra, producing a three-coordinated oxygen species, which exhibits one of the highest $\chi_Q$ values known for an unprotonated oxygen (6.5 MHz). Variation of $\delta_{iso}$, $\chi_Q$ and $\eta$ with structural parameters, particularly the Si–O–Si bond angle, has been demonstrated in the $SiO_2$ polymorphs, and subsequently used to infer structural information from silica-based glasses. Such correlations have also been used to determine the reliability and accuracy of *ab initio* calculations. In addition, $^{17}O$ NMR has been employed to follow the first-order $\alpha$–$\beta$ phase transition in quartz which occurs at 527 K, providing information on Si–O–Si bond angle changes and the dynamic averaging to cubic symmetry occurring in the $\beta$ phase.

Mueller *et al.* demonstrated the use of $^{17}O$ DAS and DOR in the study of isotopically-enriched magnesium and calcium silicate minerals.[26] They were able to resolve inequivalent

oxygen species (8 in the case of wollastonite, $CaSiO_3$), and extract quadrupole and chemical shift parameters for each, emphasising the differences between the bo and nbo in chain silicates. MQMAS has now also been employed to study layered aluminosilicate clay minerals, such as pyrophyllite ($Al_2Si_2O_{10}O–(OH_2)$), resolving Si–O–Si, Si–O–$^{[4]}$Al and Si–O–$^{[6]}$Al oxygen species (where the superscript denotes the aluminium coordination). Although similar chemical shifts were observed for many of the oxygens, once again the bo species exhibited substantially larger $\chi_Q$ values (4.5–5.5 MHz) than the Si–O–$^{[n]}$Al oxygens (3–4 MHz).

Magnesium silicates have a particular prominence in the Earth sciences, being the principal chemical constituent of the Earth's mantle. The major component in the Earth's upper mantle (to depths of 410 km) is olivine $\alpha$-$(Mg,Fe)_2SiO_4$, an iron-bearing form of forsterite $\alpha$-$Mg_2SiO_4$. The high resolution spectrum of forsterite, acquired by MQMAS, displays three distinct resonances with intensities in the ratio 1 : 2 : 1, corresponding to three distinct nbo species, as forsterite is an orthosilicate, containing only isolated $SiO_4$ tetrahedra.[27] Deeper in the Earth, as the pressure increases forsterite is thought to undergo phase transformations to the $\beta$- and $\gamma$- forms of $Mg_2SiO_4$, wadsleyite and ringwoodite, defining a region (410 to 660 km) known as the transition zone. To synthesise these materials isotopically enriched in $^{17}O$ is difficult, requiring pressures similar to those in the mantle, up to 20 GPa for ringwoodite. This involves the use of a multi-anvil apparatus, thereby reducing significantly the amount of sample available, often to only a few mg. In this case, the sensitivity of MQMAS, particularly under fast MAS, is not sufficient and the more sensitive STMAS technique may be required to obtain high resolution spectra. Fig. 6 shows the STMAS spectrum of $\sim$10 mg of wadsleyite ($\beta$-$Mg_2SiO_4$), recorded at 9.4 T with a spinning rate of 30 kHz.[28] The broad MAS spectrum is resolved into four distinct resonances, with intensity ratios 1 : 4 : 2 : 1. Wadsleyite is a pyrosilicate, with $Si_2O_7$ groups, and the spectrum contains one bo species, two nbos and a five-coordinate species, coordinated only by magnesium. This latter species exhibits a particularly low $\chi_Q$ resulting from the predominantly ionic nature of its bonding.

One area of particular interest in geochemistry is the ability of the nominally anhydrous minerals in the mantle to incorporate water or hydrogen into their structures. It is thought that the mantle contains a vast amount of water, perhaps many more times that in the Earth's oceans, yet relatively little is known about how or where this water may be stored. Owing to the sensitivity of the $^{17}O$ chemical shift and quadrupole parameters to the local environment, $^{17}O$ NMR offers an ideal probe for the study of both anhydrous and hydrous materials. Hydroxyl oxygens are expected to possess high $\chi_Q$ values, often between 6 and 8 MHz. MQMAS was used to study the humite minerals, $pMg_2SiO_4{\cdot}Mg(OH)_2$, proposed as models for the storage of water within olivine.[29] Although the high resolution spectra were able to identify the distinct nbo species, 4 for chondrodite ($p$ = 2) and 8 for clinohumite ($p$ = 4), the hydroxyl oxygens were not observed, probably as a result of their increased second-order broadening. However, a static $^{17}O$ spectrum revealed a much broader lineshape, similar to that of brucite $Mg(OH)_2$, in addition to the narrower resonance of the nbos. Only this broad resonance appeared when the spectrum was acquired with CP, confirming its assignment as a hydroxyl oxygen, with $\chi_Q$ of $\sim$6.8 MHz for both chondrodite and clinohumite.

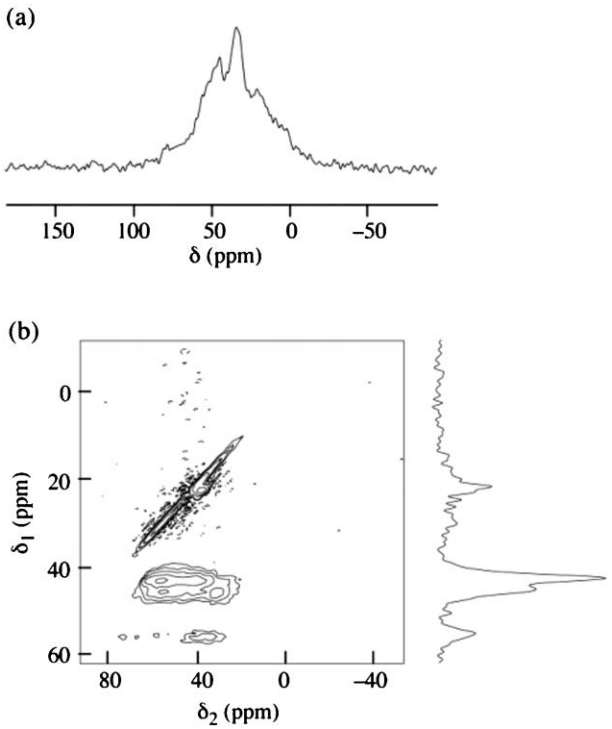


**Fig. 6** $^{17}O$ (54.2 MHz) (a) MAS NMR spectrum and (b) two-dimensional STMAS NMR spectrum and corresponding isotropic projection of NMR of $\sim$10 mg of 35% isotopically-enriched wadsleyite ($\beta$-$Mg_2SiO_4$). Reproduced from ref. 28 with permission of the copyright owner the American Chemical Society.

Many minerals have attained their structural states over geologic time and at geological conditions. However, the study of such naturally-occurring minerals is restricted (or even prohibited) by the low natural abundance of $^{17}O$. Although natural abundance spectra of simple oxides can be obtained relatively easily (Sec. 3.1), it is much more difficult to acquire spectra on more complex mineral systems, especially when $\chi_Q$ increases. It has been demonstrated that natural abundance $^{17}O$ spectra of such systems may be acquired through the use and combination of different sensitivity enhancement techniques.[30] For example, CP allows the observation of the hydroxyl oxygen species in brucite and boehmite (AlO(OH)) at natural abundance levels, providing significant sensitivity gains. For systems without $^1H$, a combination of RAPT and CPMG can provide a considerable increase in sensitivity, allowing spectral acquisition of materials such as forsterite at natural abundance levels. This approach was utilised in the study of zircon ($ZrSiO_4$), a mineral which has acquired a partially metamict structure over $\sim$570 million years through the radioactive decay of the natural uranium it contains.[30] The natural abundance $^{17}O$ RAPT/CPMG spectrum of zircon contained, in addition to the non-bridging Si–O–Zr oxygens at $\sim$150 ppm, a considerable amount of bridging (Si–O–Si) oxygen species at $\sim$65 ppm, resulting from the damage of the structure by the recoil of heavy nuclei that have emitted alpha particles.

 

### 3.3 $^{17}$O NMR of zeolites

Zeolites are a family of framework aluminosilicate materials, based on networks of corner sharing $AlO_4$ and $SiO_4$ tetrahedra, producing channels, cavities and pores of molecular dimensions. This has resulted in their use as heterogeneous catalysts, drying agents, ion-exchange materials and molecular sieves, and the study of zeolites has, therefore, generated great interest. One aspect of importance is the ordering of Al and Si within the tetrahedral units. The extent of this ordering has a great effect upon the temperature and conditions of zeolite formation and upon chemical reactivity. In general, it is assumed, particularly for zeolites with Si/Al $\geqslant 1$ that an aluminium avoidance rule, 'Lowenstein's rule', holds, with Al–O–Al linkages forbidden or disfavoured. A second, and perhaps more important, aspect of zeolite study is the binding (both position and strength) of extra framework cations and adsorbed molecules. The latter is of particular importance for the understanding of the application of zeolites as heterogeneous catalysts. There has been a great deal of $^{27}$Al and $^{29}$Si NMR study of zeolitic frameworks,[1] but relatively little $^{17}$O NMR. However, although $^{27}$Al and $^{29}$Si NMR may help to determine framework ordering, it is often to the oxygens that adsorbed species bind. Therefore, $^{17}$O NMR enables detailed study of this binding and, through the sensitivity of the chemical shift and quadrupolar parameters to the local environment, provides a probe of framework structure and order. Many zeolites may be enriched in $^{17}$O through simple hydrothermal exchange, although owing to differences in reactivity of the various oxygen species, care should be taken when interpreting relative peak intensities.

Early $^{17}$O NMR of zeolites (one-dimensional static and MAS experiments)[31] demonstrated that the $^{17}$O $\chi_Q$ was particularly sensitive to the nature of the local oxygen environment. Clear differences were observed between Si–O–Al ($\chi_Q$ of 3–4 MHz) and the more covalent Si–O–Si species ($\chi_Q$ of 5–6 MHz). However, the low resolution of these experiments often results in considerable overlap of resonances, limiting the information available. In particular, no resolution of crystallographically-distinct Si–O–Si or Si–O–Al species was observed. The introduction of high resolution techniques has renewed interest in $^{17}$O NMR of zeolites, and DAS, DOR and MQMAS have all been employed to produce high resolution spectra of a variety of zeolitic materials. The removal of the second-order quadrupolar broadening allows easy distinction of Si–O–Al and Si–O–Si species. However, despite this increase in resolution, it is still often not possible to distinguish individual crystallographically-distinct species. This may result from the large number of such oxygen species in the framework and, in some cases, the presence of a range of local environments. In many zeolites, the Si/Al disorder within the tetrahedra produces a range of local coordination environments (*e.g.*, different second and fourth nearest neighbours) for a particular oxygen. When combined with differences in M–O–M′ bond angles and differing interactions with extra framework cations, this may result in a distribution of chemical shifts for a particular oxygen and a broadening of the high resolution spectrum.

In some cases, however, resolution of distinct crystallographic species is possible. This is often the case for highly siliceous zeolites where the local oxygen environment is very similar, with little Si/Al disorder, and few or no extra framework cations. Resolution of distinct oxygen species was achieved in siliceous ferrierite[15] with MQMAS (14.1 T), producing five distinct resonances exhibiting differing intensities. The combination of this with variable field (11.7 to 18.8 T) DOR was able to prove the presence of ten distinct oxygens (Fig. 7). A full assignment of the spectrum was hindered by the complexity of the system, the non-quantitative nature of MQMAS, the need to interpret and integrate the complex spinning sideband patterns of DOR, possible site-selective enrichment and the limits of the size of the cluster that could be accurately calculated.

Resolution of distinct species can be possible in aluminosilicate zeolites, particularly when Si/Al $\approx 1$. In this case, the

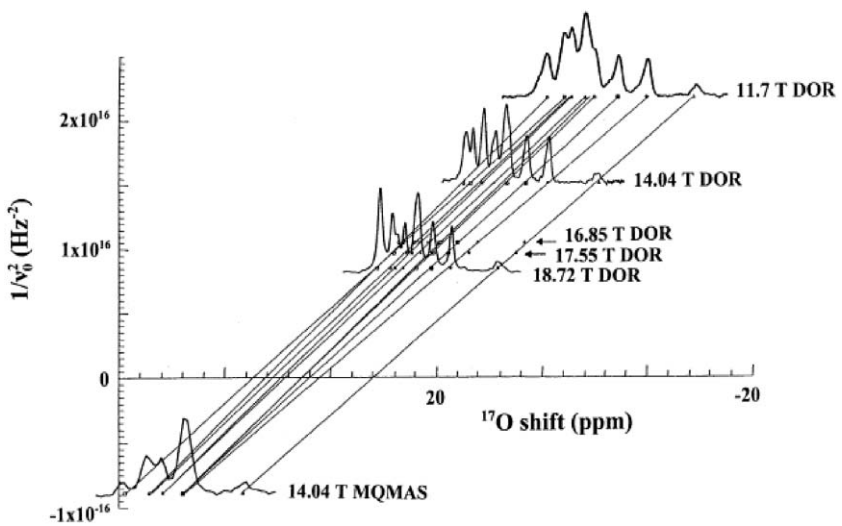


**Fig. 7** Combination of $^{17}$O DOR data for ferrierite at five magnetic fields with MQMAS data. The intercept on the x-axis corresponds to the isotropic chemical shift for each site and the gradient is proportional to the quadrupolar product $P_Q$. Reproduced from ref. 15 with permission of the copyright owner the American Chemical Society.

'ordering' of the aluminosilicate framework (produced by the preference for aluminium avoidance) reduces the range of possible local environments and, therefore, distributions in chemical shift. Pingel *et al.*[32] demonstrated resolution of three crystallographically-distinct Si–O–Al species in hydrated Na-exchanged zeolite A using MQMAS. The three sites possessed very similar $\chi_Q$ ($\sim$3.4 MHz) but different isotropic chemical shifts. Similar resolution was also demonstrated for the four oxygen species in zeolite Na–LSX (Si/Al $\sim$ 1). Based upon these results a correlation of $^{17}O$ isotropic chemical shift with Si–O–Al bond angle was suggested, with the shift decreasing as the angle increased. However, no such simple correlation was observed for the Si–O–Si species in ferrierite.[15] More detailed work on a range of ion-exchanged zeolites (both hydrated and dehydrated)[33] demonstrated that although the M–O–M′ angle does affect the chemical shift, no simple general correlation is possible as a result of the presence of extra framework species. Bonding to cations or to water can have a dramatic effect upon the $^{17}O$ chemical shift, with a shift of $\sim$34 ppm observed for one oxygen between Na–A and Tl–A, for example.

It is also possible to follow the exchange kinetics of zeolite frameworks by $^{17}O$ NMR, as was demonstrated for stilbite.[34] Stilbite is a naturally-occurring zeolite (with Si/Al = 3) and can be enriched in $^{17}O$ by hydrothermal exchange with enriched $H_2O$. Using MQMAS, DAS and DOR, clear separation of Si–O–Si and Si–O–Al resonances was observed, but owing to a distribution of chemical shifts resolution of individual crystallographically-distinct species was not obtained. However, it was shown that when the zeolite was back reacted, *i.e.*, heated with unenriched water, differences were observed in the relative intensities of the two resonances, indicating that the Si–O–Al oxygen species reacted more quickly. Furthermore, in some stilbites, a third resonance was also observed, as shown in the MQMAS spectrum in Fig. 8,[34] and was assigned to Al–O–Al oxygen species. The formation of this type of linkage is unusual in zeolites with Si/Al $\geqslant$ 1, owing to the preference for aluminium avoidance. The Al–O–Al oxygen was shown to have a relatively large $\chi_Q$, of 3.8 MHz, greater than the $\chi_Q$ values observed in many simple aluminate species, and an isotropic shift of $\sim$21 ppm. It was estimated to account for 1% of the oxygen in the zeolite framework. This resonance showed a considerable decrease in intensity when back reacted with unenriched water, reflecting its high reactivity and, hence, its more unfavourable formation.

Catalytic properties of zeolites centre on the acid sites within the structure. The direct detection of Si–(OH)–Al Brønsted sites has only recently been reported.[35] For zeolite HY, although the $^{17}O$ resonance associated with the Brønsted site could not be unambiguously identified in the direct MAS experiment, its presence was revealed using high field in combination with CP, double resonance REDOR and transfer of population by double resonance (TRAPDOR) experiments. The $^{17}O$ parameters deduced were $\chi_Q$ = 6.6 MHz, $\eta$ = 0.8 and $\delta_{iso}$ = 28 ppm, where $\chi_Q$ is significantly larger than is normally associated with Si–O–Al linkages. On reaction with acetone, which is known to interact with the zeolite framework *via* the Brønsted site, a significant decrease in the $\chi_Q$ to $\sim$5 MHz was observed. This can be translated into a lengthening of the O–H bond length from 0.97 to 1.02 Å. Hence, $^{17}O$ NMR offers much promise as a sensitive and subtle probe of Brønsted acidity in such materials and understanding the structural geometry of the active sites.

### 3.4 Glasses

In glasses the structure at the most local level (*i.e.*, nearest neighbour) very closely resembles that observed in related crystalline phases. This was clearly demonstrated by $^{29}Si$ MAS NMR, which revolutionised the characterisation of silicate-based glasses through the identification of the different local $Q^n$ species.[1] Also from $^{17}O$ NMR, for example for $SiO_2$, the $^{17}O$ NMR interaction parameters of a silica glass very closely match the values seen from the crystalline silica polymorphs quartz and cristobalite, being related to the fundamental $SiO_4$ building block of the structure. The key difference between a crystal and a glass is the disorder created by the way these $SiO_4$ units are joined together to form the extended network structure in the system. In $SiO_2$ glasses the Si–O–Si linkages

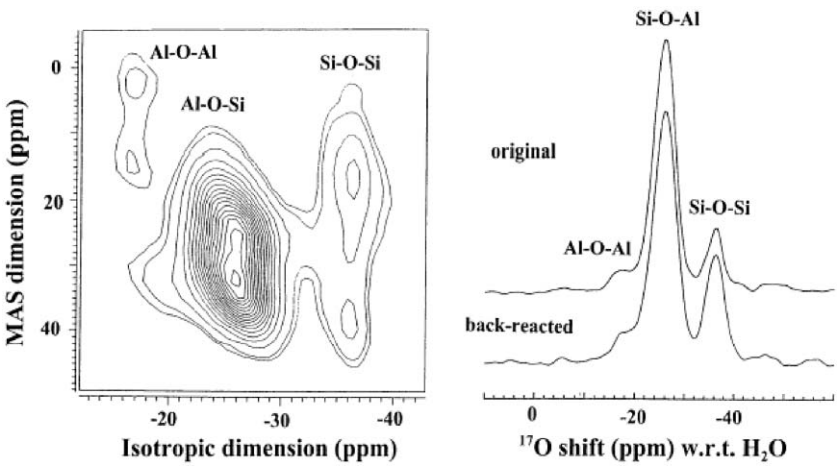


**Fig. 8** $^{17}O$ 3Q MAS NMR spectrum of the zeolite stilbite, showing at right the projections of the isotropic dimension of the 3Q MAS spectra of the original isotopically-enriched sample, and after back-reaction with isotopically normal water vapour. Reproduced from ref. 34 with permission of the copyright owner the Mineralogical Society of America.

 

show a distribution of bond angles, and it is this distribution that is a strong characteristic of the intermediate range order. The key here is to be able to relate the NMR parameters to this bond angle distribution. Although $^{29}$Si chemical shifts show variation due to the changes in the bond angle at the oxygen they are not directly at the site where the variation is occurring and the effect on the $^{29}$Si shift is an average effect over the 4 corners. A much more direct probe of this bond angle variation is to look at the $^{17}$O. There has been much theoretical effort in trying to relate the observed parameters to the bond angle distribution, particularly by Grandinetti and co-workers.[36] The bond angle distributions have been extracted in some detail for both $SiO_2$ and $GeO_2$ glass.

In multi-component glasses the possibilities for disorder increase. For example, with the addition of network modifiers to a simple silicate glass charge balance within the system is achieved by the formation of nbos. In the $^{17}$O NMR spectra from such glasses using a combination of static, MAS, DAS and MQMAS data, the bo and nbo can be characterised by their NMR parameters and the intensity of each signal, with changes in the $^{17}$O parameters associated with them reflecting changes in the internal structure. For example, changing the alkali cation shows an effect on both the maximum in the bond angle distribution and its width. In such metal silicate glasses the intermediate range order is then determined by both the Si–O–Si bond angle distribution and the ordering of the cations. Cation ordering has profound implications for many properties of a glass, such as the configurational entropy of the system and transport properties. $^{17}$O NMR can provide information on both the change in the bond angle distribution and the cation ordering, with the nbo being particularly sensitive to coordination (and hence changes) by the metal. Comparison of the isotropic dimension of the DAS spectra of $K_2Si_4O_9$ and $KMg_{0.5}Si_4O_9$ glasses showed no significant increase in width in the mixed cation glass, but the peak position was shifted from the position in the pure potassium glass.[37] There is still some dispute as to the implications of this observation with originally it being suggested that a high degree of cation ordering was occurring with the nbo atoms probably coordinated by two potassiums and one magnesium, whereas other studies have interpreted this as favouring Mg only distributions around the nbo. In other systems the intensity of the 3QMAS and DAS data is more closely modelled by a random distribution of cations. A comparison of potassium tetrasilicate glasses quenched under ambient and $\sim$6 GPa pressures showed an increase in the mean bond angle for the pressure-formed sample.

A further level of complication comes when additional network formers or intermediates are also present in the system, since then there is an additional factor that can produce disorder in the structure, namely the ordering of the network forming cations. Given the importance of crystalline aluminosilicates in the Earth sciences (see Sec 3.2) aluminosilicate glasses are also important especially as models of melt structure. In aluminosilicates a key question for glasses and melts is whether or not the aluminium avoidance principle that is generally found in crystalline materials applies. Consider albite ($NaAlSi_3O_8$) glass where each $AlO_4^-$ is charge balanced by an $Na^+$ so that the glass network should be completely connected (*i.e.*, $Q^4$). The question then is the degree of ordering of the silicon and aluminium within the network, which in principle can have Si–O–Si, Si–O–Al and Al–O–Al contributions. From a 3Q MAS study of albite it was clear that there were only Si–O–Si and Si–O–Al contributions (Fig. 9(a)) and the ratio was within error the expected 1 : 1 for an ordered network with no Al–O–Al groups.[38] Calibration of $^{17}$O parameters from Al–O–Al links in some aluminates where these are the only bridging groups, allowed the NMR interaction parameters, and hence their position in MQMAS spectra, to be deduced. There is probably strong overlap of the Al–O–Al and Al–O–Si peaks in 3Q MAS spectra so that detection of a few % Al–O–Al may be difficult.[39] Borosilicates are important technological glasses and the long-standing $^{11}$B NMR approach for characterising such materials is being supplemented by $^{17}$O to separate the B–O–B, Si–O–B and Si–O–Si groups, along with the nbo present in the system. It appears from initial $^{17}$O work that the borate and silicate parts of the network are quite intimately mixed with intensities reflecting almost random ordering. The $^{17}$O MQMAS data and its analysis has become much more sophisticated for such systems, with now in borosilicates separate $^{17}$O signals being detected from nbo, Si–O–Si, Si–O–$^{[4]}$B, Si–O–$^{[3]}$B, $^{[4]}$B–O–$^{[3]}$B and $^{[3]}$B–O–$^{[3]}$B. Hence detailed, quantitative information is available on the fragments that make up the structure.

In aluminoborate glasses exactly the same type of information is available with the additional factor that the aluminium can take [4], [5] and [6] coordination. There is increasingly extensive data from crystalline model compounds and other simpler glasses such that the parameters from the different contributions are becoming much better defined. In a recent example of sodium aluminoborate glasses up to six different contributions were fitted (Fig. 9(b)).[40] The $^{17}$O NMR data obtained for some of these groups can be cross-checked against the $^{11}$B and $^{27}$Al NMR data collected from the same glasses. There are a number of models that can be used to calculate the oxygen distribution between the different environments, with two of the most straightforward random mixing or maximum $^{[4]}$M–O–$^{[4]}$M avoidance within the constraints of composition. Analysis of the data for sodium aluminoborate glasses indicated that the distribution was far from random (Fig. 9(c), (d)). It also suggested that $^{[4]}$Al–O–$^{[4]}$B formation is favoured over homonuclear tetrahedral groups. The data also suggested that the oxygen associated with the $^{[5,6]}$Al–O–$^{[4]}$Al linkages is probably tricoordinate.[40]

### 3.5 Sol–gel produced materials

Sol–gel routes have become an important approach for materials chemistry, allowing many novel materials, including organic–inorganic hybrids, to be produced that would be difficult or impossible by other approaches. In this route precursors are mixed in solution which then, *via* a series of reactions, cross-link to form a network that increases in extent until it gels. The final product is then formed by heating this gel to give a solid, usually porous network, where the unwanted parts of the precursor materials (*i.e.*, residual organic fragments or hydroxyls) have largely been removed. A key part of the condensation process is the nature of the oxo

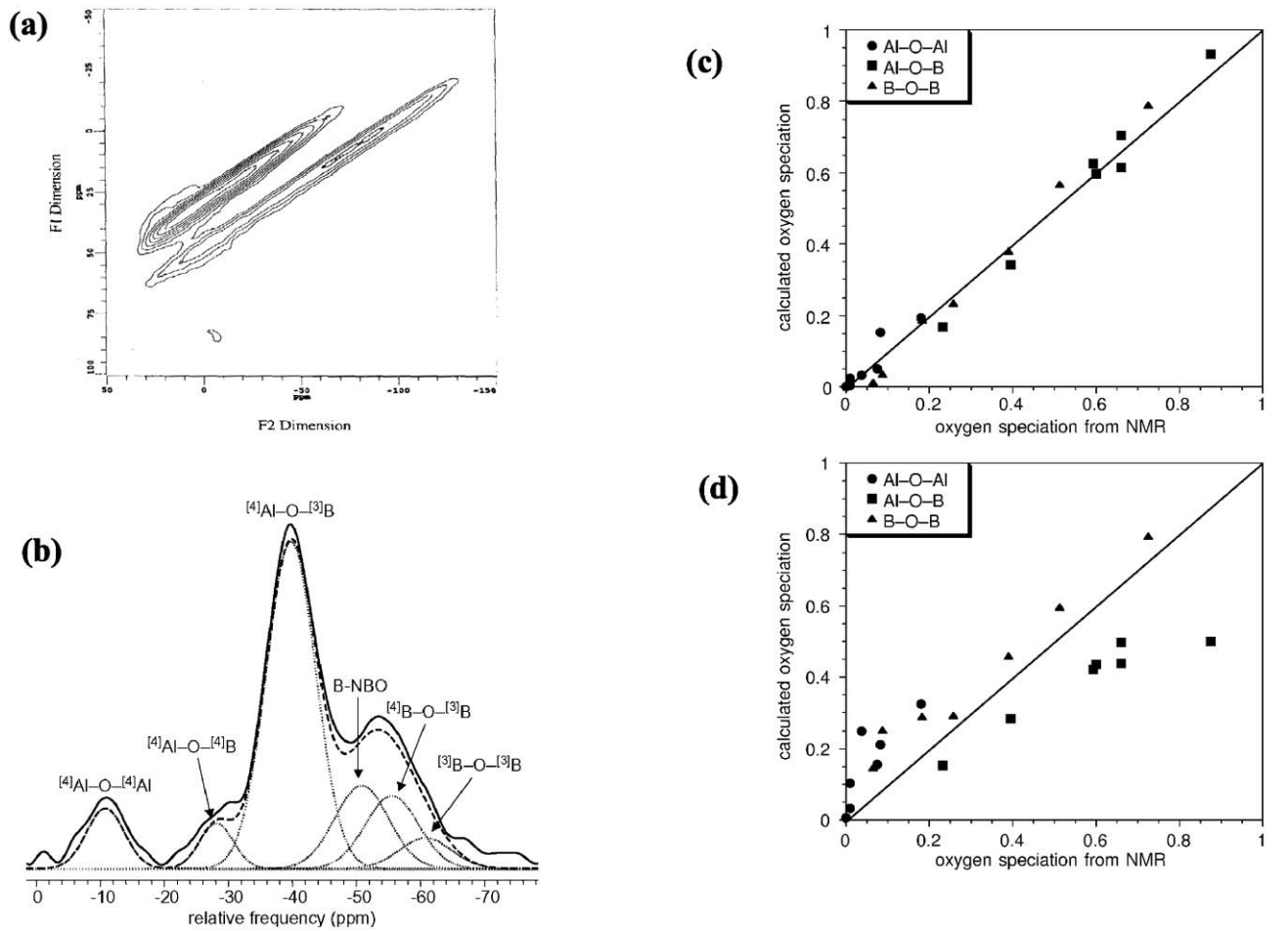


**Fig. 9** Examples of $^{17}O$ 3Q MAS NMR spectra from multicomponent glasses (a) showing the complete resolution of Si–O–Si and Si–O–Al fragments in albite glass and (b) the 3Q MAS isotropic projection from an aluminborate glass with 6 distinct contributions with the intensity distribution of the different components for tetrahedral unit avoidance (c) and a random distribution (d). These figures are reproduced from ref. 38 (part (a)) and ref. 40 (parts (b)–(d)) with permission of the copyright owner Elsevier Science.

bridges formed and the level of chemical homogeneity in multi-component systems. As seen for glasses $^{17}O$ is a very high quality, discriminatory probe of the oxygen distribution between the different fragments. Now significant background studies of the sol–gel formation of simple binary oxides have been carried out and the shift ranges associated with many M–O–M bridges have been deduced and these have been extensively reviewed in Sec 6.3.2 of ref. 1. A spin-off from these studies defining the shift ranges of the different fragments is that the details of the structural rearrangements of the intermediate states formed during the heating process of these oxide gels have been deduced. A whole range of different structural changes occur with the detail subtly depending on the nature of each oxide. Another point that rapidly emerges from these observations is that because of the large chemical shift range that $^{17}O$ exhibits, often simple MAS spectra are observed, even at moderate field that allow all the fragments present to be resolved. As an example, sol–gel formed $TiO_2$ has been studied in detail and the structural development is controlled by the hydrolysis ratio and by the use of complexing agents.[41] The nature of the ligand was found to change the local structural units in the titania core. In gel-produced materials of this type the linewidths are largely determined by chemical shift dispersion, such that broader lines are indicative of a wider range of environments and hence a more disordered structure.

A key technological problem when different components with differing reaction rates are mixed is the extent to which mixing of those different components occurs and how this is maintained with heat treatment. This question is of importance for both the structure and the properties of the material formed. The formation of nanocrystalline $TiO_2$-doped $SnO_2$ directly occurs in the rutile structure and does not proceed *via* the anatase phase as it would for pure $TiO_2$. A $^{17}O$ MAS NMR spectrum showed by the presence of a peak at 595 ppm that the rutile structure forms in the very early stages of the reaction. In addition, the tin has to be integrated within the main structure rather than being a separate nanophase as there were no resonances in the region of $SnO_2$.

A more significant problem for binary gels occurs when one component is $SiO_2$. Here there is a crucial question as to what extent is the added oxide mixed with the $SiO_2$ or phase separated. Just as with glasses, different resonances from the different fragments need to be identified. The most studied

 

problem is mixed $TiO_2$–$SiO_2$ where for the most part the added $TiO_2$ is the minority component. Then distinct resonances can be seen, well separated in the MAS NMR spectra, from Ti–O–Ti, Ti–O–Si and Si–O–Si. The presence of Ti–O–Si indicates that at least to some extent there must be atomic mixing, and if this is observed in the absence of Ti–O–Ti then it must indicate that the titanium is dispersed in the silica network. At low concentrations (<15 mol% $TiO_2$) only Si–O–Si and Ti–O–Si are observed, with the Ti–O–Ti only being seen at concentrations where phase separation is expected.[42] For a whole range of metal oxides added to $SiO_2$ these different fragments can be observed and hence the phase separation behaviour examined. The interesting comparison is that below ~15 mol% added metal oxide, in the region of complete solid solution with $SiO_2$ (*i.e.*, there is no sign of the formation of M–O–M linkages), there is significant variation in the $Q^n$ speciation revealed by $^{29}$Si MAS NMR. This is an indication that although the samples are all effectively homogeneous the role the added metal is playing within the silica network is very different. The metals fall into two groups, those which form a high fraction of $Q^4$ (*e.g.*, Ti, Nb) and those which form a spread of $Q^n$ species (*e.g.*, Zr, Ta, Hf). The difference has been ascribed to the coordination which the metal can take. For the former group the metal is becoming tetrahedrally coordinated as part of the actual framework itself and hence bridging bonds form, whereas the other metals take higher coordinations and create nbos.

The $^{17}$O NMR work on sol–gel prepared materials has now advanced beyond just oxide-based systems to hybrid metal oxide–siloxane materials. Here the silicon functionality changes such that the four bonds of the silicon atoms can be to varying numbers of oxygens and carbons. Again $TiO_2$ additions have been the most commonly studied with all the different links readily identified. The $^{17}$O signals from Si–O–Si fragments showed a ~40 ppm down field shift reflecting the changed electron density around the central silicon in progressing from the normal $SiO_4$ unit to $SiO_2C_2$.[43] In more complex systems where there is a mixture of such functionality 3Q MAS has been used to discriminate and quantify the number of oxygens bridging between differently functionalised silicons (*i.e.*, $O_3Si$–O–$SiO_3$ will give a different position to $CO_2Si$–O–$SiO_2C$) and hence the degree of mixing between the different silicons can be accurately monitored.[44]

### 3.6 Phosphates

Reports of $^{17}$O solid state NMR from oxygens that are attached to phosphorus are still quite sparse. In phosphates with isolated $PO_4^{3-}$ units all the oxygens are non-bridging and then $\chi_Q$ of 4–5 MHz are typical. The shifts can discriminate different P–O bond lengths, with as an example in $CaHPO_4.H_2O$ the P–O bond lengths are 1.69, 1.58, 1.69 and 1.34 Å and the $^{17}$O MQ MAS spectrum showed two lines in the ratio 3 : 1. In microporous aluminophosphates (AlPOs) the $\chi_Q$ observed to date are typically ~5.6–5.7 MHz. A key experiment for $^{17}$O NMR on phosphates, particularly glasses, would be to discriminate bo (P–O–P) and nbo (P–O–M). A big step forward has been the observation of the $^{17}$O NMR signals from $P_2O_5$.[45] In $P_2O_5$ there are both bridging and terminal oxygen sites, and the terminal oxygens have a smaller $\chi_Q$ of ~4 MHz compared to the bridging oxygens which have $\chi_Q$ ~ 7.5 MHz. Such large values only really become accessible with high fields and fast MAS. In phosphate glasses several studies have shown that the number of bo and nbo is consistent between the $^{31}$P and $^{17}$O derived NMR data. Just as with silicates this has now been further extended to multi-component glasses such as sodium borophosphates and it is clear that P–O–B links play a key role in these materials.

### 3.7 Hydroxyl oxygen species

The observation and characterisation of hydroxyl (OH) oxygen species is of considerable interest in the study of a wide range of materials, including glasses, sol–gels and minerals, owing to the importance of quantifying levels of hydration and the investigation of hydrogen bonding. A fairly wide range of parameters for hydroxyl oxygen species has been reported; for example, isotropic chemical shifts range from −20 to 30 ppm for typical Mg–O–H species, 40–50 ppm for Al–O–H species and up to 60–80 ppm for many Ca–O–H species.[46]

In many alkali and alkaline earth hydroxides there is a high degree of covalency to the OH bond, resulting in relatively large $\chi_Q$ values, typically in the range 6–8 MHz.[46] For the case of Al–O–H linkages, $\chi_Q$ values in the region of 5–6 MHz have been observed for simple hydroxides and oxyhydroxides, although larger values (up to 7 MHz) have been observed in aluminosilicate minerals.[46] These large $\chi_Q$ values result in broad resonances which may be difficult to observe under MAS (particularly at slow speeds or low $B_0$ field strengths), and in many cases static echo spectra have been employed. Alternatively, the observation of hydroxyl oxygens has been achieved by the use of cross-polarisation (CP) from $^1$H which selectively enhances any oxygen resonances which are spatially close to $^1$H nuclei[10] as described in Section 3.2 for humite minerals[29] and boehmite.[30] Cross-polarisation signal intensity depends strongly on the OH distance and so in some cases (usually where a pair of nuclear spins are fairly isolated) quantitative information can be obtained. Observation of these hydroxyl species with large $\chi_Q$ is also difficult by MQMAS where the signal intensity decreases as $\chi_Q$ increases, hindering the accuracy of quantitative interpretation. Relative enhancements in signal intensity have been achieved (for example, in boehmite[47]) using two-dimensional techniques which combine MQMAS and CP.

Different types of hydroxyl species were observed by van Eck *et al.*[46] in sol–gel produced silica. Their observation and characterisation was difficult owing to overlap in the spectrum with the resonance assigned to the Si–O–Si oxygen. A range of $\chi_Q$ values was shown to be present, with many species having very small (<200 kHz) $\chi_Q$. The OH signal was characterised by a very short $T_1$ relaxation time (~0.1 ms), and a short $T_2$, restricting the use of static echo experiments. It was suggested that this results from high mobility of the hydroxyl hydrogen, creating rapidly fluctuating interactions (*e.g.*, dipolar, quadrupolar) which strongly enhance the oxygen relaxation. This is substantiated by the observation that proton decoupling has

little effect and that CP is very inefficient, in contrast to the efficient CP observed for the relatively rigid hydroxyls discussed above. Such motion also has implications for the observation of these hydroxyl species by MQMAS, where the excitation of multiple-quantum coherences is also inefficient when $\chi_Q$ is very small. In these silica gel materials MQMAS spectra only showed evidence for a small subset of the hydroxyl species, those where motion was presumably slower, with larger $\chi_Q$ values of 2.8–3.2 MHz.

The observation and accurate quantification of hydroxyl species in glasses is of considerable importance, as the level of glass hydration has significant implications for many of its physical and chemical properties. An important question involves the mechanism of the interaction of water with the glass, *i.e.*, whether any network bonds are broken (forming species such as Si–O–H and Al–O–H) or whether only exchange of cations for $H_2O$ takes place. A study of hydrous aluminosilicate glasses[48] revealed significant changes to the $^{17}O$ NMR spectrum upon the addition of water. In particular, a peak corresponding to $H_2O$ was observed, with a fairly large $\chi_Q$, while the chemical shift showed a strong dependence upon the nature of the charge balancing cation (*i.e.*, $Na^+$ or $K^+$), suggesting significant cation–$H_2O$ interaction. In addition, MQMAS spectra revealed a loss of intensity associated with more reactive Al–O–Al linkages, though no breaking of the network Si–O–Si and Si–O–Al bonds was observed. The Al–O–H species produced by such loss of Al–O–Al linkages could not be directly observed, assumed to be as a result of either a large range of chemical shifts and large $\chi_Q$ values or as a consequence of hydrogen motion.

A well-resolved Si–O–H (silanol) oxygen species was observed in the spectrum of potassium hydrogen silicate[49] (a model compound for hydrous silicate glasses), with a chemical shift of 60 ppm and a $\chi_Q$ (3.5 MHz) similar to that found in calcium silicate gels. Whilst smaller than that found in the alkali/alkali earth silicates this value is larger than the small $\chi_Q$ observed in the sol–gel materials, perhaps implying that rapid $^1H$ motion is not predominant. The characterisation of this species (and in particular its position) demonstrate that the loss of $^{17}O$ nbo signal observed in pure alkali silicate glasses upon hydration is a purely a result of the overlap of the silanol hydroxyl signal with that of the bridging O species and little or no disruption to the framework structure is produced.

### 3.8 Other ceramic phases

The use of $^{17}O$ NMR to study ceramic phases has largely been covered under a number of the above sections, but some cases have not been considered in these. Two examples that should be mentioned are in oxynitride ceramics, where clearly distinguishable signals could be observed from the nbo and the 'ionic' oxygens, *i.e.*, those that are only bonded directly to the metal ions in the system. Increasing the radius of the cation increases the isotropic shift of the oxygen.[50] In high temperature oxide-based ceramic superconductors oxygen is at the core of the structure. The oxygen shift and relaxation has provided important clues as to the charge correlations and dynamics in such materials[1,51] and continues to be widely used today.

## 4. Summary

This review has given an overview of the background of the methodological developments of solid state NMR that have been behind the great increase in resolution of NMR spectra from non-integer spin quadrupolar nuclei. This has given impetus to studies using solid state $^{17}O$ NMR over the last decade. Examples showing the wide range of applications in chemical science, and the types of information that it can provide are taken from several different applications to inorganic materials. Increasingly extensive data sets of $^{17}O$ parameters are being collected. The large variation in both $\chi_Q$ and $\delta_{iso}$ (Fig. 10) shows that $^{17}O$ NMR is a very sensitive probe of local structure. The data collected in Fig. 10(a) show that correlation suggested (eqn 1) more than 20 years ago still reflects well the general trend, although the details could usefully be revisited. The shift range for a given fragment

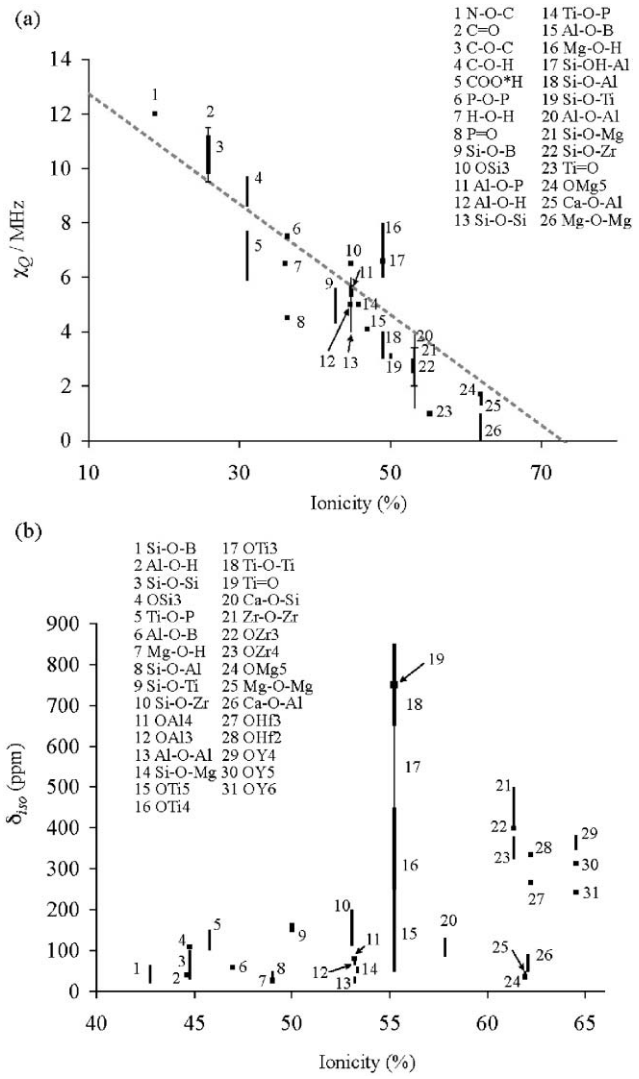


**Fig. 10** Summary of some $^{17}O$ quadrupole coupling constants ($\chi_Q$) and isotropic chemical shifts ($\delta_{iso}$) as a function of the bond ionicity (as defined in eqn 2) for various M–O–M′ fragments showing the large range of values. The dashed line in (a) shows the trend described by eqn 1 for comparison.

(*e.g.*, Ti–O–Ti) can show a large variation that is sensitive to the actual coordination of the oxygen (Fig. 10(b)). It is hoped that this review will encourage new researchers to embark on using $^{17}$O solid state NMR in their research.

## Acknowledgements

SEA thanks the Royal Society for the provision of a Dorothy Hodgkin Fellowship and EPSRC, the research councils for an RCUK Academic Fellowship and the Leverhulme Trust for funding work on $^{17}$O NMR. MES thanks EPRSC, BBSRC and the Royal Society for funding projects based around $^{17}$O NMR. MES also thanks the EPSRC and the University of Warwick for partial funding of NMR equipment. The authors are very grateful to all of their collaborators who have been a source of inspiration in developing projects using $^{17}$O.

## References

1 K. J. D. Mackenzie and M. E. Smith, *Multinuclear Solid-State NMR of Inorganic Materials,*Pergamon, Oxford, 2002 and references therein.
2 S. Schramm, R. J. Kirkpatrick and E. Oldfield, *J. Am. Chem. Soc.*, 1983, **105**, 2483–2485.
3 S. Schramm and E. Oldfield, *J. Am. Chem. Soc.*, 1984, **106**, 2502–2506.
4 V. Lemaitre, M. E. Smith and A. Watts, *Solid State Nucl. Magn. Reson.*, 2004, **26**, 215–235.
5 M. R. Hampson, S. Allen, I. J. King, C. J. Crossland, P. Hodgkinson, R. K. Harris, F. Fayon and J. S. O. Evans, *Solid State Sci.*, 2005, **7**, 819–826.
6 P. N. Gunawidjaja, M. A. Holland, G. Mountjoy, D. M. Pickup, R. J. Newport and M. E. Smith, *Solid State Nucl. Magn. Reson.*, 2003, **23**, 88–106.
7 M. E. Smith and E. R. H. van Eck, *Prog. Nucl. Magn. Reson. Spectrosc.*, 1999, **34**, 159–201 and references therein.
8 K. J. Pike, V. Lemaitre, A. Kukol, T. Anupõld, A. Samoson, A. P. Howes, A. Watts, M. E. Smith and R. Dupree, *J. Phys. Chem. B*, 2004, **108**, 9256–9263.
9 S. E. Ashbrook and S. Wimperis, *Prog. Nucl. Magn. Reson. Spectrosc.*, 2004, **45**, 53–108.
10 T. H. Walter, G. L. Turner and E. Oldfield, *J. Magn. Reson.*, 1988, **76**, 106–120.
11 D. Massiot, F. Fayon, M. Capron, I. King, S. Le Calve, B. Alonso, J. O. Durand, B. Bujoli, Z. H. Gan and G. Hoatson, *Magn. Reson. Chem.*, 2002, **40**, 70–76.
12 M. Bak, J. T. Rasmussen and N. C. Nielsen, *J. Magn. Reson.*, 2000, **147**, 296–330.
13 C. J. Pickard and F. Mauri, in *Calculation of NMR and EPR Parameters: Theory and Applications*, ed. M. Knaupp, Wiley-VCH, Weinheim, 2004, and references therein.
14 J. A. Tossell, *Phys. Chem. Miner.*, 2004, **31**, 41–44 and references therein.
15 L. M. Bull, B. Bussemer, T. Anupõld, A. Reinhold, A. Samoson, J. Sauer, A. K. Cheetham and R. Dupree, *J. Am. Chem. Soc.*, 2000, **122**, 4948–4958.
16 P. Blaha, K. Schwarz, P. Sorantin and S. B. Trickey, *Comput. Phys. Commun.*, 1990, **59**, 399–415.
17 M. Profeta, M. Benoit, F. Mauri and C. J. Pickard, *J. Am. Chem. Soc.*, 2004, **126**, 12628–12635.
18 C. Gervais, R. Dupree, K. J. Pike, C. Bonhomme, M. Profeta, C. J. Pickard and F. Mauri, *J. Phys. Chem. A*, 2005, **109**, 6960–6969.
19 T. J. Bastow and S. N. Stuart, *Chem. Phys.*, 1990, **143**, 459–467.
20 T. J. Bastow, P. J. Dirken, M. E. Smith and H. J. Whitfield, *J. Phys. Chem.*, 1996, **100**, 18539–18545.
21 P. A. Thomas, A. Baldwin, R. Dupree, P. Blaha, K. Schwarz, A. Samoson and Z. H. Gan, *J. Phys. Chem. B*, 2004, **108**, 4324–4331.
22 M. R. Hampson, P. Hodgkinson, J. S. O. Evans, R. K. Harris, I. J. King, S. Allen and F. Fayon, *Chem. Commun.*, 2004, 392–393.
23 M. R. Hampson, J. S. O. Evans and P. Hodgkinson, *J. Am. Chem. Soc.*, 2005, **127**, 15175–15181.
24 H. K. C. Timken, S. E. Schramm, R. J. Kirkpatrick and E. Oldfield, *J. Phys. Chem.*, 1987, **91**, 1054–1058.
25 P. J. Grandinetti, J. H. Baltisberger, I. Farnan, J. F. Stebbins, U. Werner and A. Pines, *J. Phys. Chem.*, 1995, **99**, 12341–12348.
26 K. T. Mueller, Y. Wu, B. F. Chmelka, J. Stebbins and A. Pines, *J. Am. Chem. Soc.*, 1991, **113**, 32–38.
27 S. E. Ashbrook, A. J. Berry and S. Wimperis, *Am. Mineral.*, 1999, **84**, 1191–1194.
28 S. E. Ashbrook, A. J. Berry, W. O. Hibberson, S. Steuernagel and S. Wimperis, *J. Am. Chem. Soc.*, 2003, **125**, 11824–11825.
29 S. E. Ashbrook, A. J. Berry and S. Wimperis, *J. Am. Chem. Soc.*, 2001, **123**, 6360–6366.
30 S. E. Ashbrook and I. Farnan, *Solid State Nucl. Magn. Reson.*, 2004, **26**, 105–112.
31 H. K. C. Timken, G. L. Turner, J. P. Gilson, L. B. Welsh and E. Oldfield, *J. Am. Chem. Soc.*, 1986, **108**, 7231–7235.
32 U. T. Pingel, J. P. Amoureux, T. Anupõld, F. Bauer, H. Ernst, C. Fernandez, D. Freude and A. Samoson, *Chem. Phys. Lett.*, 1998, **294**, 345–350.
33 D. Freude, T. Loeser, D. Michel, U. Pingel and D. Prochnow, *Solid State Nucl. Magn. Reson.*, 2001, **20**, 46–60.
34 J. F. Stebbins, P. D. Zhao, S. K. Lee and X. Cheng, *Am. Mineral.*, 1999, **84**, 1680–1684.
35 L. M. Peng, Y. Lui, N. J. Kim, J. E. Readman and C. P. Grey, *Nat. Mater.*, 2005, **4**, 216–219.
36 T. M. Clark and P. J. Grandinetti, *Solid State Nucl. Magn. Reson.*, 2005, **27**, 233–241 and references therein.
37 I. Farnan, P. J. Grandinetti, J. H. Baltisberger, J. F. Stebbins, U. Werner, M. A. Eastman and A. Pines, *Nature*, 1992, **358**, 31–35.
38 P. J. Dirken, S. C. Kohn, M. E. Smith and E. R. H. van Eck, *Chem. Phys. Lett.*, 1997, **266**, 568–574.
39 J. F. Stebbins, J. V. Oglesby and S. K. Lee, *Chem. Geol.*, 2001, **174**, 63–75.
40 L. S. Du and J. F. Stebbins, *Solid State Nucl. Magn. Reson.*, 2005, **27**, 37–49.
41 E. Scolan, C. Magnenet, D. Massiot and C. Sanchez, *J. Mater. Chem.*, 1999, **9**, 2467–2474.
42 P. J. Dirken, M. E. Smith and H. J. Whitfield, *J. Phys. Chem.*, 1995, **99**, 395–401.
43 C. Gervais, F. Babonneau and M. E. Smith, *J. Phys. Chem. B*, 2001, **105**, 1971–1977.
44 F. Babonneau, C. Bonhomme, C. Gervais and J. Maquet, *J. Sol–Gel Sci. Technol.*, 2004, **31**, 9–17.
45 B. R. Cherry, T. M. Alam, C. Click, R. K. Brow and Z. H. Gan, *J. Phys. Chem. B*, 2003, **107**, 4894–4903.
46 E. R. H. van Eck, M. E. Smith and S. C. Kohn, *Solid State Nucl. Magn. Reson.*, 1999, **15**, 181–188.
47 S. E. Ashbrook and S. Wimperis, *J. Magn. Reson.*, 2000, **147**, 238–249.
48 J. V. Oglesby, P. Zhao and J. F. Stebbins, *Geochim. Cosmochim. Acta*, 2002, **66**, 291–301.
49 J. V. Oglesby, S. Kroeker and J. F. Stebbins, *Am. Mineral.*, 2001, **86**, 341–347.
50 R. K. Harris, M. J. Leach and D. P. Thomson, *Chem. Mater.*, 1992, **4**, 260–267.
51 A. Rigamonti, F. Borsa and P. Carretta, *Rep. Prog. Phys.*, 1998, **61**, 1367–1439.